(BL1B)

One-Photon Photoionization Thresholds of Aromatic Molecules on Water Surface in Ambient Condition

Teiichiro Ogawa[A], Shin-ya Sasaki[A], Manabu Tokeshi[B], and Takanori Inoue[A]

[A]*Department of Molecular Science and Technology, Kyushu University*
Kasuga-shi, Fukuoka, 816-8580
[B]*Falculty of Engneering, The University of Tokyo,*
Hongo, Tokyo, 113-1111

Photoionization behavior at the solution surface is different from that in the bulk solution. Photoionization threshold in solution has been determined in a single-photon process using synchrotron radiation or hydrogen discharge lamp, and in a two-photon process using laser radiation. Although there are a few measurements on photoionization threshold of aromatic molecules on solution surface using laser two-photon excitation, no measurements have been carried out using one-photon excitation on solution surface. We have tried to measure one-photon ionization spectra (wavelength dependence of photoionization efficiency) and photoionization thresholds of aromatic molecules on water surface using synchrotron radiation.

The experimental apparatus is shown in Fig.1. Synchrotron radiation of wavelength from 160 to 240 nm was used as an excitation source. The beam power was 10^{10} photons/sec as monitored using a photomultiplier to calibrate its wavelength dependence. The beam was not focused and irradiated the solution surface horizontally. The solution was kept in a stainless-steel vessel (0.5mL) of 1.5 cm in diameter, and the vessel was served as the current collecting electrode. A disk electrode was located 5 mm above the solution surface and was connected to a high-voltage power supply unit. The photoionization current was measured using a current amplifier(Keithley, 617). The perylene, pyrene and methylanthracene (guaranted grade, Nacalai Tesque) were used without further purification. The water was distilled, deionized, filtered and distill again in a quartz vessel.

The one-photon ionization spectra have been measured for the three molecules on the water surface. The blank signal (signal of pure water) was relatively small and negligible. The photoionization of perylene on water surface in the concentration range between 10^{-6}M – 10^{-8}M has showed linear dependence on concentration. The photoionization spectrum was normalized by beam power and solution concentration.

The photoionization current near threshold can be represent by a power law,

$$I = c\,(E_{excess})^{5/2} = c(h\nu - I_{th})^{5/2}$$

where E_{excess} is the excess energy of the ionized pair, $h\nu$ is the photon energy and I_{th} is the ionization threshold. A plot of the (2/5)th power of the normalized photoionization current versus the photon energy should give a straight line, and its onset on the abscissa should give I_{th}, because there would be no photoionization current below I_{th}. Figure 2 shows the photoionization spectrum for the three aromatic molecules on water surface, and I_{th} of perylene, pyrene, and methylanthracene have been determined to be 6.0, 6.3 and 5.9 eV, respectively. I_{th} of perylene was determined to be 5.95 eV by a two-photon process using a Ti-sapphire laser and agree with the present value within experimental errors.

The photoionization threshold on the surface has been related with the ionization potential in gas phase, I_p, as:

$$I_{th} = I_p + P^+,$$

where P^+ is the polarization energy of the positive ion. This equation should be applicable to these molecules in this study, because the electron escapes directly from the surface and so the electron affinity of the solvent is able to be negligible. P^+ of perylene on water can be determined as –0.9eV. The value of P^+ can be obtained from Born equation using the dielectric constant and the radius of the molecule. The observed value of P^+ was about half as much as the calculated value, this indicates that the effective dielectric constant of water surface should be much smaller than that of bulk water, 80.4 at 20°C.

Reference

1. Inoue, T.: Masuda, K.: Nakashima, K.: Ogawa, T., *Anal.Chem.*, 66(1994)1012.
2. Watanabe, I.: Ono, K.: Ikeda, S., *Bull.Chem.Soc.Jpn.*, 64(1991)352.
3. Ogawa, T.: Chen, H.: Inoue, T.: Nakashima, K., *Chem.Phys.Lett.*, 229(1994)328.
4. Born, M., *Z.Physik*, 1(1920)45

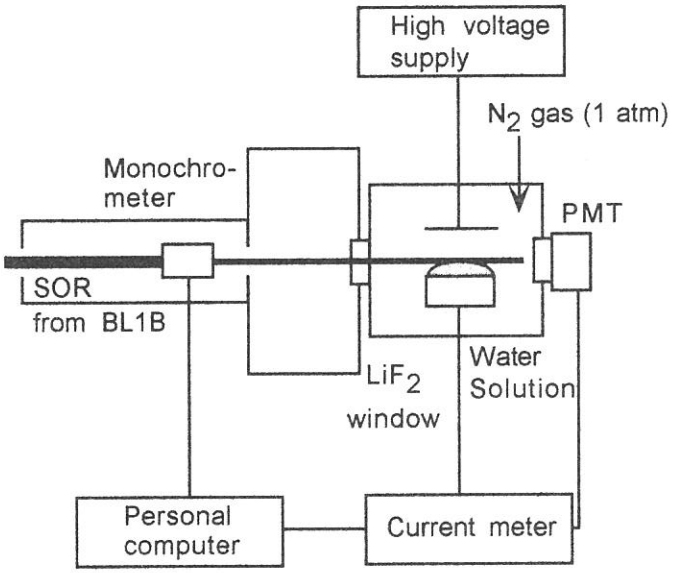

Fig.1 Schematic diagram of the experimental appatus

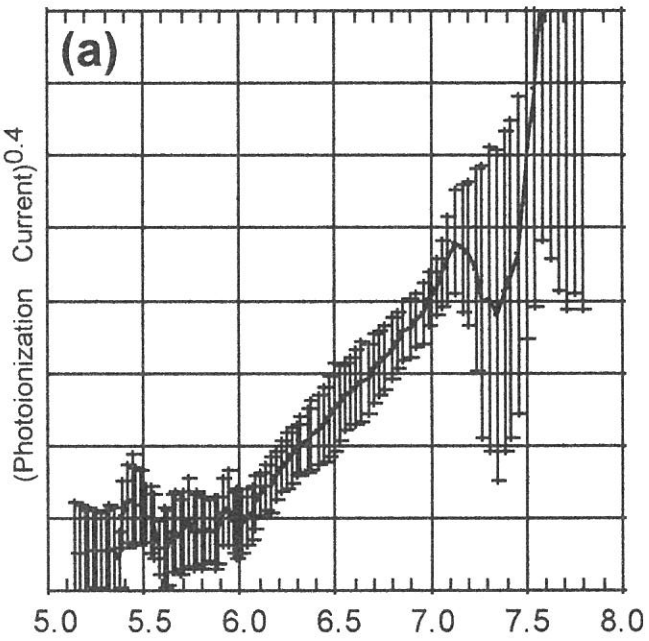

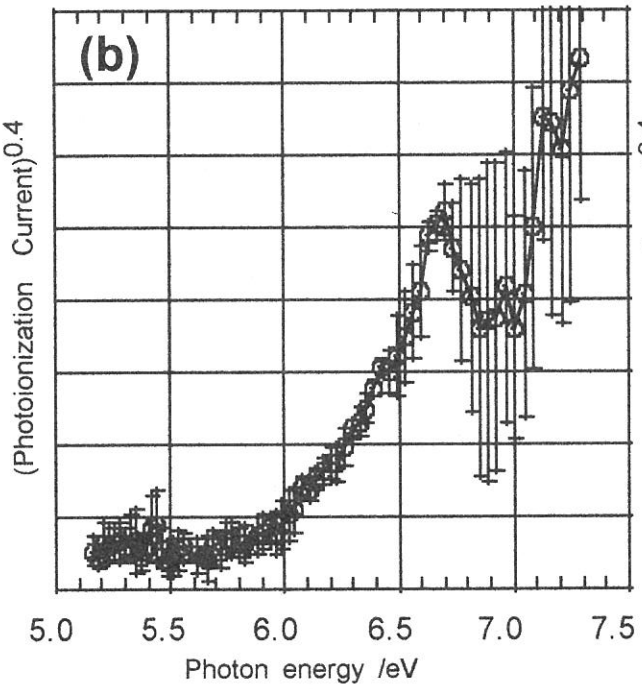

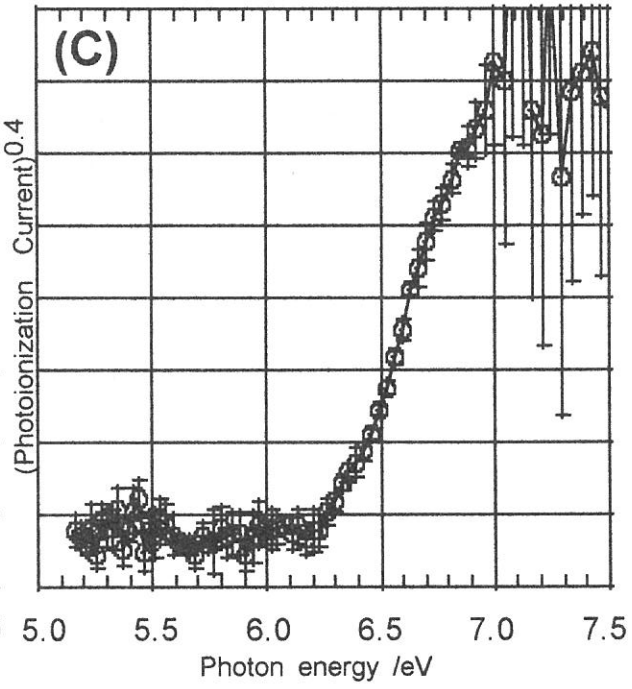

Fig.2 Photoionization current spectra of (a) perylene, (b) methylanthracene, (c) pyrene.

(2B1) SELECTION OF ORIENTED OXYGEN ADMOLECULES ON A PT(133) STEPPED SURFACE

Manami Sano, Yoshiyuki Seimiya, Yuichi Ohno, Tatsuo Matsushima, Shin-ichiro Tanaka[A] and Masao Kamada[A]

Catalysis Research Center and Graduate School of Environmental Earth Science, Hokkaido University, Sapporo 060-0811, Japan

[A] Institute for Molecular Science, Myodaiji Okazaki 444-0867, Japan.

Oxygen admolecules on Pt(133)=(s)3(111)x(111) were characterized with thermal desorption (TDS) and near edge X-ray absorption fine structure (NEXAFS). Three desorption peaks from the admolecules are found at 150 K (α_3-O_2), 170 K (α_2-O_2) and 220 K (α_1-O_2). The admolecules due to α_1-O_2 lie along the step edge. The α_2-O_2 axis is rotated significantly from the trough direction. α_3-O_2 on the terrace is more rotated. The admolecules with different orientations can be separately prepared on this surface.

A typical TDS spectrum of the oxygen desorption from the molecular adsorption states is shown in Fig. 1. α_1-O_2 was concluded to be located on or near the step, because it is suppressed completely by preadsorbed atomic oxygen. On the other hand, α_2-O_2 and α_3-O_2 are on the declining (111) terrace because their desorption is hardly affected by oxygen adatoms on the step. α_2-O_2 is suppressed by preadsorbed oxygen populated on the terrace. The α_3-O_2 desorption increases with increasing amount of oxygen atoms except for a high coverage range. α_3-O_2 is far from the step sites.

NEXAFS spectra were obtained at 110 K for modified surfaces by atomic oxygen which yielded each of the three α-O_2 species in the subsequent heating. Oxygen adatoms were present on the pre-treated surface and a remarkable electron yield was found around 530 eV, as shown in Fig. 2 (a). Therefore, the spectra were examined in the differential form between raw spectra and those of oxygen adatoms in the same amount. The orientation of the electric vector, E, of the X-ray, θ, is measured from the surface parallel in a plane parallel to the trough.

Only the σ^* resonance appears at $\theta = 0^\circ$ in the spectra of α_1-O_2. However, with increasing θ, the σ^* resonance fades and the π^* resonance grows rapidly. Moreover, the σ^* resonance disappears completely in a wide angle range, when E is perpendicular to the trough. α_1-O_2 is oriented along the trough. The two other α-O_2 species show different angle dependence. In the spectra of α_3-O_2, both π^* and σ^* states of resonance appear at $\theta = 0^\circ$ as shown in Fig. 2 (b). This molecule appears to be rotated from the trough direction.

The rotation angle was determined from a simple simulation of the angle dependence of the relative intensity of both resonance signals. Each peak area was determined by curve fitting using two Gaussian functions as indicated by the broken curve. In the simulation, the molecular axes of all the species were assumed to be parallel to the surface plane, in accord with HREELS work. As shown in Fig. 3, we concluded that the admolecule yielding α_1-O_2 lies along the step edge, whereas α_2-O_2 and α_3-O_2 lie on the declining (111) terraces and are inclined 35~45° and 50~60° from the trough direction, respectively.

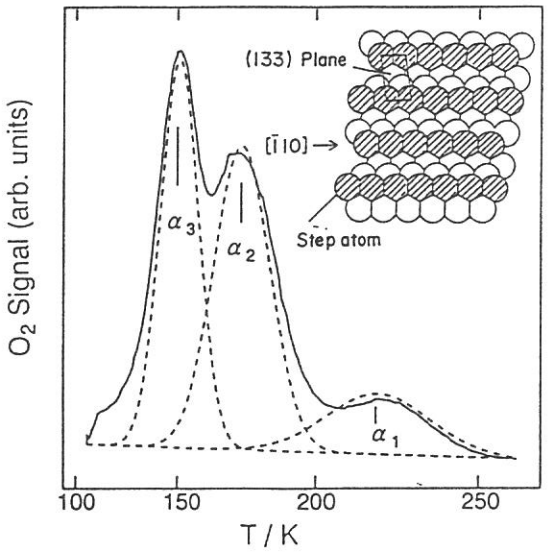

Fig. 1 A TDS spectrum of oxygen admolecules. The surface structure is inserted.

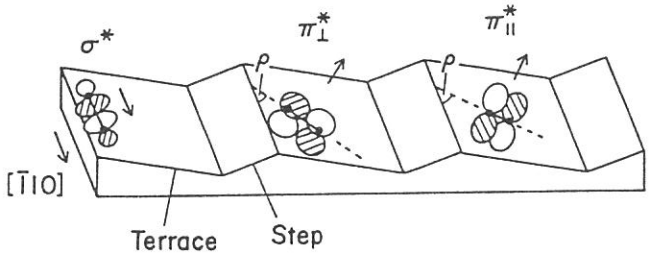

Fig. 3 Molecular and orbital orientation. ρ defines the rotation angle of the molecular axis.

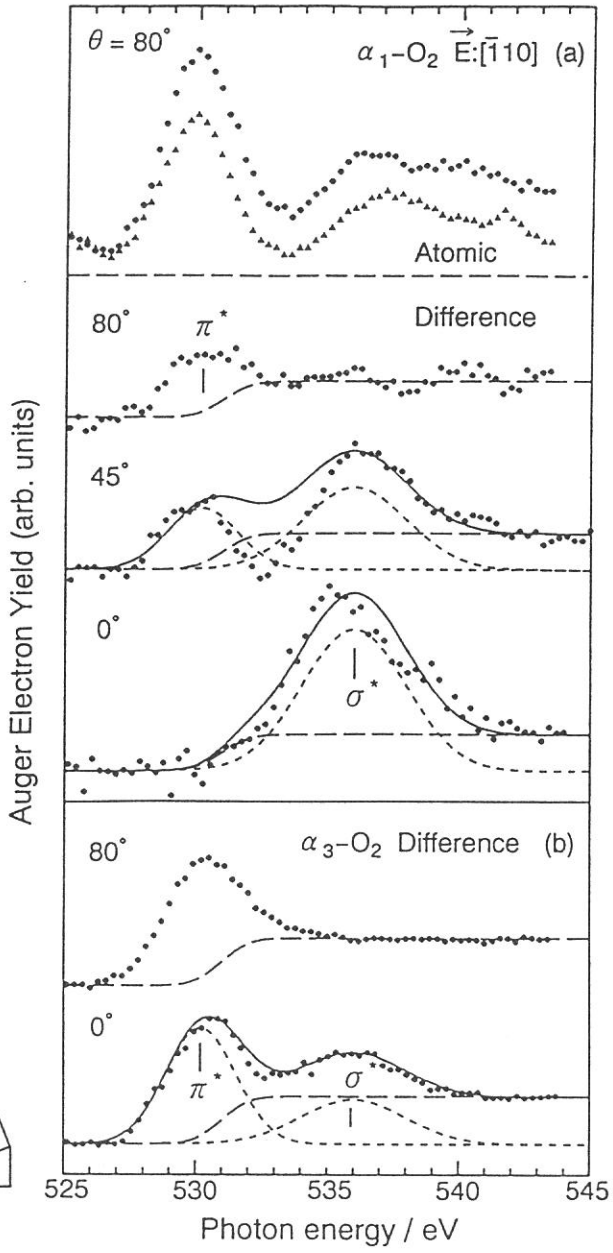

Fig. 2 NEXAFS spectra of (a) α_1-O_2 and (b) α_3-O_2. The X-ray electric vector is in a plane in the [1̄10] direction.

(BL2B1)

ELECTRONIC STRUCTURES IN THE VALENCE REGION OF CHEMISORBED AND PHYSISORBED SPECIES ON Pd(110)

Jun Yoshinobu[1,2], Maki Kawai[1], Shin-ichiro Tanaka[3], Kazuo Watanabe[3], Yoshiyasu Matsumoto[3,4] and Masao Kamada[3]

1) The Institute of Physical and Chemical Research (RIKEN), 2-1 Hirosawa, Wako 351-01. 2) The Institute for Solid State Physics, The University of Tokyo, 7-22-1 Roppongi, Minato-ku, Tokyo 106. 3) Institute for Molecular Science, Myodaiji-cho, Okazaki 444. 4) The Graduate University for Advanced Studies, Shonan village, Hayama, Kanagawa 240-01.

When an atom or a molecule is adsorbed on a metal surface, discrete electronic energy levels are chang due to the interaction with the surface. In the case of weak interaction, adsorbate-induced levels are shifted to lower energy and broadened [1]. This broadening is referred as adsorbate-induced resonance. If the interaction is very strong, the broadened band will be split into a pair of a bonding state below valence band and an antibonding state at the top of valence band. This case may be relevant for chemisorption on transition metals which are characterized by a narrow d-band in addition to a broad sp-band.

As a typical model for molecular chemisorption, the valence electronic structure (in particular, near the Fermi level) of adsorbed CO on metal surfaces is still of interest and a controversial subject. There are two models for extreme cases; (1) the surface complex model (the Blyholder model [2]), where a σ-bond is formed between the CO 5σ molecular orbital (MO) and a metal d-orbital (donation) and also a π-bond between the CO 2π MO and a metal d-orbital (back-donation). (2) the surface resonance model [3,4], where the unoccupied 2π state is shifted and broadened due to the interaction with metal bands. Since the low energy side of the resonance is located below the Fermi energy (EF), this region is bonding in character.

We have investigated the electronic structures of CO, CH_4 and Xe on Pd(110) by means of photoelectron spectroscopy (PES) using UVSOR BL2B1 in Institute of Molecular Science. In order to enhance the sensitivity for the adsorbate-derived states in valence PE spectra, photon energy at the Cooper minimum (hν = 120-130 eV) was utilized.[5-7] In the case of the CO saturated Pd(110) surface at 90 K, peaks are observed at ~3.4 eV, 8.0 eV (with a shoulder at ~7.2eV), 11.0 eV and 14.4 eV below the Fermi level (EF). In addition to the previously reported peaks (1π & 5σ at ~8 eV and 4σ at ~11 eV),[8] two peaks were newly observed. The 3.4 eV peak could be assigned to the bonding state hybridized between CO 2p and Pd 4d orbitals. The 14.4eV peak is tentatively assigned to the CO 4s shake-up satellite. In the "physisorption" systems, i.e., CH_4 and Xe on Pd(110), only the smooth attenuation of photoemission from the Pd 4d band was observed in the PE spectra.[9] The study is to be published.[10]

[1] B. I. Lundqvist, H. Hjelmberg and O. Gunnarsson, in: Photoemission and the electronic properties of surfaces (John Wiley & Sons, New York, 1978).
[2]G. Blyholder, J. Phys. Chem., 68 (1964) 2772.
[3]B. Gumhalter, K. Wandelt, and Ph. Avouris, Phys. Rev. B 37 (1988) 8048.
[4]Ph. Avouris, Physica Scripta., 35 (1987) 47.
[5]J.W. Cooper, Phys. Rev., 128 (1962) 681.
[6]P.S. Wehner, S.D. Kevan, R.S. Williams, R.F. Davis and D.A. Shirley, Chem. Phys. Lett., 57 (1978) 334.
[7]E. Miyazaki, I. Kojima, M. Orita, K. Sawa, N. Sanada, T. Miyahara and H. Kato, Surf. Sci. 176(1986) L841.
[8]H. Conrad, G. Ertl, J. Küppers and E.E.Latta, Disc. Farad. Soc. 58 (1974) 116.
[9]K. Jacobi and and H.H. Rotermund, Surf. Sci., 133 (1983) 401.
[10]J. Yoshinobu, M. Kawai, S. Tanaka, K. Watanabe, Y. Matsumoto and M. Kamada, J. Electry. *in press.*

(BL2B1)

Study of Site-Specific Ion Desorption from a Si(100) Surface Saturated by Fluorine Using Photoelectron Photoion Coincidence Spectroscopy

Kazuhiko Mase, Sinya Hirano, Shin-ichiro Tanaka, and Tsuneo Urisu

Institute for Molecular Science, Okazaki 444-8585, Japan

Since a core-electron is localized at an atom, site-specific fragmentation is expected to be induced by core-electron excitations. Site-specific fragmentation is important not only as the fundamental science of molecular dynamics but also as the fundamental technology of the reaction control for the new material production. Photoelectron photoion coincidence (PEPICO) spectroscopy is an ideal tool for site-specific ion desorption study because it provides ion mass spectra of the sites related to the selected photoelectrons [1]. In the present article, we describe a study of site-specific ion desorption from a Si(100) surface saturated by Fluorine at the room temperature (Si(100)-F).

Figure 1 shows PEPICO spectra of Si(100)-F. PEPICO F^+ signal was observed for Si:2*p* photoelectron with kinetic energies of 101 eV. Figure 2 shows potoelectron spectra (PES) and potoelectron energy dependence of the PEPICO F^+ yield (PEPICO F^+ yield spectrum). The peak position and shape of the PEPICO F^+ yield spectrum was observed to be similar to those of the difference PES between Si(100)-F and a clean Si(100) surface, which corresponds to the ≡SiF, $=SiF_2$, and $-SiF_3$ species. These results directly verify that F^+ ion desorption is induced by Si:2*p* photoionizations at the ≡SiF, $=SiF_2$, and $-SiF_3$ sites on the surface.

References

[1] S. Nagaoka *et al.*, *J. Chem. Phys.*, **107**, 10751 (1997); K. Mase *et al.*, *Surf. Sci.* **377-379**, 376 (1997).

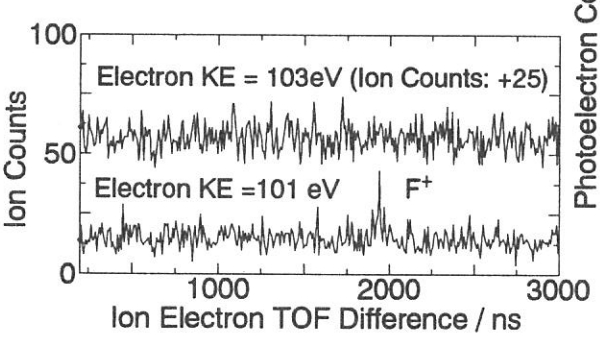

Figure 1. PEPICO spectra of Si(100)-F in coincidence with Si:2*p* photoelectron with kinetic energies of 101 eV and 103 eV.

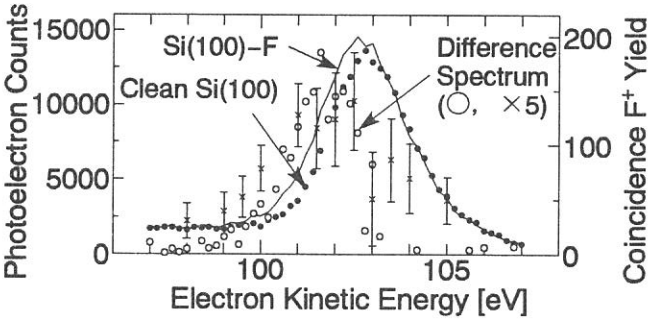

Figure 2. PES of Si(100)-F (dot line) and a clean Si(100) surface (solid line). The open circles denote the difference PES between Si(100)-F and Si(100). The crosses with an error bar denote a PEPICO F^+ yield spectrum.

(BL2B1)

Surface-NEXAFS and photo-stimulated ion desorption spectra at the C-K and O-K edges of the CO/Si(100) surface

S. Tanaka, M. Mase, M. Nagasono and M. Kamada

Institute for Molecular Science, Okazaki, 444-8585, Japan

The interaction of carbon monoxide (CO) with the solid surfaces is one of test cases for the gas-surface interaction study, and has been extensively studied on the many kinds of solid surfaces. However, only few studies have been made on the Si surface, although the surface chemistry of the Si has been attractive by the viewpoint of not only the pure science but also the technological application. In this report, we show the NEXAFS and photo-stimulated desorption spectra of CO adsorbed on the Si(100) surface at 80K, and discuss about the bonding orientation of CO on the Si(100) surface.

All the experiments were carried out at the UHV chamber at BL2B1 of UVSOR. For the measurements of the surface sensitive NEXAFS (Near-Edge X-ray Absorption Fine Structure) spectroscopy, the Auger electron yield method was used, in which the yield of the Auger electron yield of the atoms of adsorbates (C-KVV for C-K edge, and O-KVV for O-K edge) were measured as a function of the photon energy. The photo-stimulated ion desorption spectra were observed by detecting the total (positive) ion yield. The Si(100) wafer was cleaned by the resistive heating in the UHV. The sample was cooled by liquid nitrogen all through the experiments. The CO-exposure was made by the use of the dosing system of pulse valve. The pressure of the gas reservoir was about 0.8 Torr, the time of the opening was 10 msec, and the doses were made for 10 times. They were enough to make the surface saturated with CO, and all the results reported here are for the the Si(100) surface with 1 mono-layer of CO.

Figure 1 shows the NEXAFS spectra of the CO/Si(100) surface at the C-K edge as a function of the incident angle of the photons. The angle from the surface normal was 60° and 20° for the upper and lower curves, respectively. It was difficult to estimate the difference of the efficiency of the photoelectron detection two spectra, and the intensities of the spectra were normalized by the intensity of the first peak at the threshold. The photon energy is shown referred from the energy position of the first peak for convenience. The spectra observed are similar to the NEXAFS spectra of the CO-adsorbed metal surfaces, and the first peak are ascribed to the transition to the π* resonance state, and the broad peak around 20 eV for the upper curve is ascribed to the transition to the σ* shape resonance. The intensity of the σ* shape resonance was too small to be observed in the spectrum taken at 20° of the photon incidence. Considering the polarization of the incident photons and symmetry of the molecular orbital, it is interpreted as that the CO axis on the Si(100) surface is aligned near to the surface

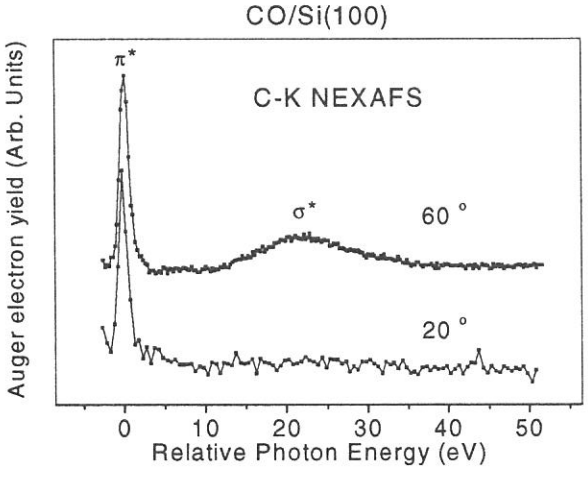

Figure 1

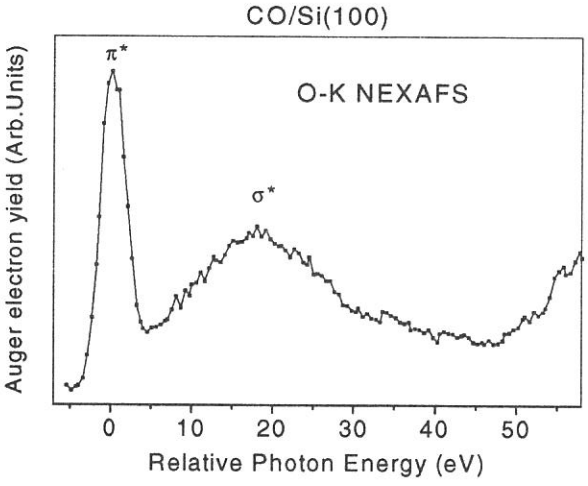

Figure 2

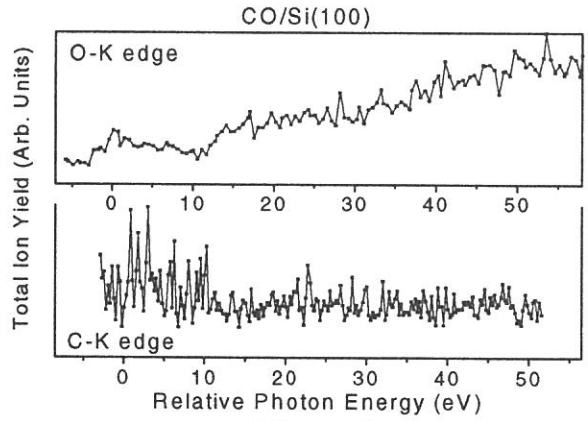

Figure 3

normal. Ho et.al. concluded that CO is bonded to the dangling bond of the Si(100) surface, and the angle of the molecular axis is about 18.6° from the surface normal, which is consistent with our observation. It is noted that it is difficult to discuss quantitatively the angle of the molecular axis, partly because the lack of the detailed data, and partly because the ambiguity of the azimuth of the Si(100)(2x1) surface.

Figure 2 shows the NEXAFS spectra at O-K edge of CO/Si(100). The incident angle of the photons was 60°. Two peaks are observed and ascribed to π^* and σ^* resonance as well as C-K edge. The peaks are broader than those in the spectrum for C-K edge because of poorer resolution of the instruments at higher energies. The enhancement at >50 eV is due to the direct excitation of photoelectrons, and not the NEXAFS signal.

Figure 3 shows the total ion yield spectra for C-K edge and O-K edge from CO/Si(100). At the O-K edge, the increase of the ion yield is observed at about 0eV, 10eV and 25 eV. The increase of the ion yield at 0eV was not reproducible, and may be due to the H^+ desorption from the ice layer adsorbed on the surface during the experiment. The increases at 10 eV and 35 eV are corresponding to the σ^* excitation and the shake-up excitation, respectively, and are similar to the case of CO adsorbed on the metal surface. The desorbing species for the CO/metal are O^+, and it is reasonable to assume a similar photon-induced dissociation takes place on the Si(100) surface. Meanwhile, no structure was observed for the ion yield at the C-K edge. It indicates that the CO molecule adsorbs on the Si(100) surface via the C atom. In this configuration, if a core hole is created at the C atom, the screening due to the electrons at the substrate will be very quick because the C atom is directly bonded to the substrate, and the relaxation without any desorption will occur. Meanwhile, a core hole at the O atom, and holes at the valence level created by the Auger transition may be possible to survive during the process of the bond breaking.

In conclusion, we have measured the NEXAFS and photo-stimulated desorption spectra of CO adsorbed on the Si(100) surface at 80K, and have shown that CO is bonded nearly perpendicular to the surface via the C atom on the Si(100) surface.

(BL2B1)

Study of ion desorption induced by the core-level excitation on the CaF_2(111) surface

S. Tanaka, M. Mase, M. Nagasono and M. Kamada

Institute for Molecular Science, Okazaki, 444-8585, Japan

Desorption of F^+ induced by core-level excitation with synchrotron radiation has been investigated on the CaF_2(111) film produced on Si(111). All the experiments were carried out at a UHV (base pressure was $1x10^{-10}$ Torr) chamber installed at BL2B1 of UVSOR at Institute for Molecular Science. CaF_2 was deposited from a boron nitride crucible onto a Si(111) surface, which has been cleaned by resistive heating in UHV.

Figure 1 shows partial electron (open circles) and total ion (lines) yields spectra of CaF_2(111) films at 80K in the region of the (a) F-1s and (b) Ca-2p edges. At the onset of the Ca-2p edge, ion yield is nearly proportional to electron yield [fig.1(b)], whereas it shows a clear enhancement at the first peak compared to electron yield in the region of the F-1s edge [fig.1(a)]. The first peak at the onset of the F-1s edge in the electron yield is ascribed to the core exciton [$(F\text{-}1s)^{-1}(Ca\text{-}4s)^1$], whereas the second peak to a transition into an unbound state in the conduction band (Ca-4s and Ca-3d). It was also observed that the peak around 688 eV for the ion yield was shifted by about -1.2 eV compared to that in the electron yield.

The left-hand panels of figure 2 show photoelectron spectra of CaF_2(111) at 300K taken at (a) hv=688eV [corresponding to the first peak observed in the ion yield spectra at the onset of the F-1s edge in fig.1(a)] and (b) at hv=349eV [corresponding to the first large peak at the onset of the Ca-2p edge in fig.1(b)]. The right-hand panels of figure 2 show coincidence signals between positive ions and electrons of kinetic energies which are indicated as A - D in their left-hand panels. All coincidence spectra have periodic backgrounds, which is considered to be related to the time structure of the electron bunchs in the storage ring of UVSOR, because the period in the backgrounds is the same as one cycle of the storage ring (178 ns). The peaks A and B in the photoelectron spectrum in fig. 2(a) are ascribed to the F-$KL_{2,3}L_{2,3}$, and F–$KL_1L_{2,3}$ Auger electron emissions, respectively, and the peaks C and D in fig.2(b) are to the Ca-$L_{2,3}M_{2,3}M_{2,3}$ Auger electron and Ca-3p photoelectron emissions, respectively.

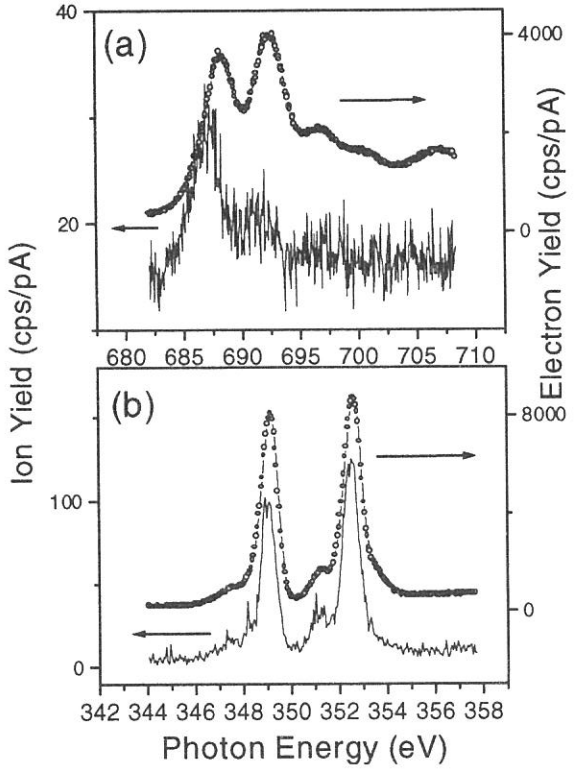

Figure 1

The electron-ion coincidence spectra [fig.2(a)] have shown clear evidence that desorption of F^+ takes place directly via a decay of the F-1s core-exciton. It is in agreement with the observation that the ion yield is enhanced compared to the electron yield at the photon energy for the F-1s core-exciton [fig.1(a)].

Meanwhile, the ion yield is nearly proportional to electron yield at the onset of the Ca-2p edge of $CaF_2(111)$ [fig.1(b)], and no peaks were observed in the coincidence spectra corresponding to the decay of the Ca-2p hole [fig.2(b)]. It indicates that the ion desorption observed in the total ion spectrum is stimulated by the secondary electron current followed by the relaxation of the Ca-2p hole.

It should be noted that the peak observed in the ion yield spectrum is shifted by about -1.2 eV compared to that in the electron yield at the F-1s edge [fig.1(a)]. It is attributed to the "surface" shift of the excitation energy for the core-exciton, because it is reasonable to assume that ion desorbs only from the surface layer, and that the ion yield predominantly reflects the electronic property at the surface in case of desorption via the direct process. Two contributions should be considered. One is an initial state contribution due to the change of binding energies of F-1s and Ca-4s levels at the surface, and the other is a final state contribution due to the change of the core-exciton binding energy at the surface. The dominant mechanism giving rise to the change in the binding energy at the surface of the ionic material is considered to be a change in the Madelung energy. According to the calculation for the $CaF_2(111)$ surface by Rotenberg et.al., the difference in the Madelung energy at the top layer consisting of F^+ and that at the second layer consisting of Ca^{2+} are about -1.05 eV and +0.3 eV, respectively, compared to the bulk value. Therefore, the photon energy for interatomic excitation at the surface is estimated to be shifted by about -1.35 eV compared to bulk, which shows rather good agreement with the observed value (-1.2eV). Accordingly, the origin of the energy shift is mainly attributed to the change in the Madelung energy at the surface of $CaF_2(111)$ film. Although there may be other contributions, e.g., a change in the core-exciton binding energy at the surface, they seem to be smaller. This may be due to the high degree of localization of the F-1s core hole.

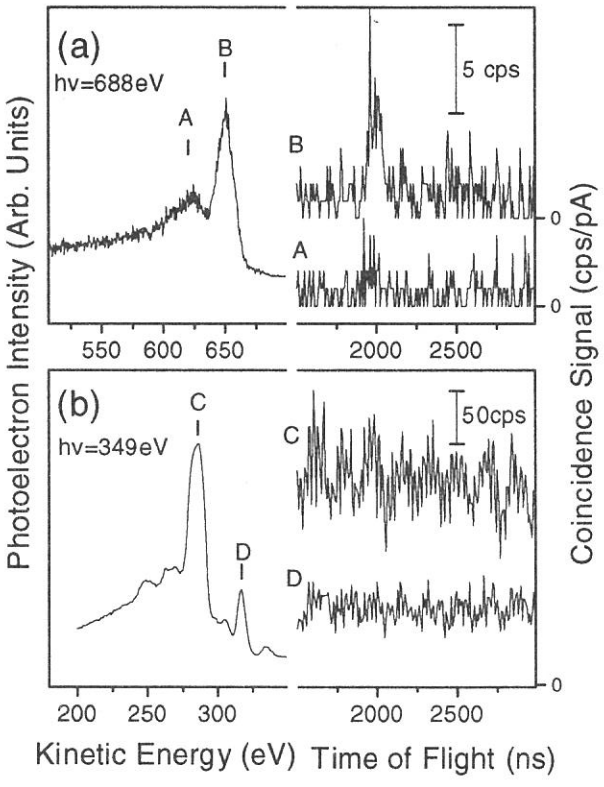

Figure 2

In summary, desorption of F^+ induced by core-level excitation with synchrotron radiation has been investigated on the $CaF_2(111)$ surface produced on Si(111). The ion yield was proportional to electron yield in the region of Ca-2p edge, while an enhancement of the ion yield was observed at the photon energy for the F-1s core-exciton. The peak corresponding to the F-1s excitation observed in the ion yield is shifted from that in the electron yield by about -1.2eV, which is predominantly ascribed to the change in the Madelung potential at the surface. The electron-ion coincidence study showed that F^+ desorption is directly stimulated via a decay of the F-1s surface core-exciton, while secondary-electron stimulated desorption is the predominant process after the creation of Ca-2p hole.

(BL2B1)

Resonant Auger Spectra of Condensed Acetonitrile Molecules Following Carbon and Nitrogen Core Excitation

Eiji Ikenaga[a], Hideki Matsuo[a], Chiaki Kato[a], Tetsuji Sekitani[a], Mitsuru Nagasono[b], Sin-ichiro Tanaka[b], Kazuhiko Mase[b], Tsuneo Urisu[b], and Kenichiro Tanaka[a]

(a) Department of Materials Science, Hiroshima University, Higashi-Hiroshima 739-8526

(b) Institute for Molecular Science, Okazaki 444-8585

Site-specific reactions have been found in photon stimulated ion desorption (PSID) induced by core excitation. The Auger stimulated ion desorption (ASID) mechanism is now proposed as a model for explanation of PSID. Recently, Mase et al. developed an electron-ion coincidence analyzer [1], and we measured Auger electron-photoion coincidence (AEPICO) spectra for condensed acetonitrile (CH_3CN) following carbon excitation [2, 3]. In the present work, we have measured resonant Auger spectra for condensed CH_3CN following carbon and nitrogen core excitation for clarifying the resonant Auger process and the ion desorption mechanism related to the Auger process. The sample was prepared by exposing a gold foil with 100L of CH_3CN at 80K.

Figure 1 shows resonant Auger electron spectra following carbon core excitation. The major contributions of the peaks were assigned on the basis of a comparison with the Auger spectra by calculation [4] and gas phase normal Auger spectra by experiment [5]. The normal Auger transition is dominant in the σ^*_{CC} and σ^*_{CN} excitation which lie above the threshold. (Fig.1e,f,g) because the excited electron promptly goes far from the parent molecule through autoionization and/or electron transfer to neighboring molecules. Auger spectra are drastically changed at the π^*_{CN} and C-H* excitation from the normal Auger spectrum (Fig.1b,d,g). The peak X is attributed to the participant Auger transition. Other peaks are attributed to the spectator Auger transition of carbon 1s. The difference in AES between the π^*_{CN} excitation and the C-H* excitation can be explained as follows: At the π^*_{CN} excitation, the transition of a C1s(CN) electron to the π^*_{CN} orbital occurs rather than that of the C1s(CH_3) electron to π^*_{CN} because the π^*_{CN} orbital is localized on the CN group. Then the spectator Auger transition which makes holes at the orbital localized on the CN group occurs selectively. In the case of the C-H* excitation, the C1s(CH_3) electron to C-H* orbital transition mainly occurs, so that the spectator Auger transition which makes holes at the orbital localized on the CH_3 group occurs selectively.

Figure 2 shows resonant Auger spectra following the nitrogen core excitation. Auger electron spectra are different from that of the carbon core excitation. At the π^*_{CN} excitation (Fig.2b), spectral feature except for the peak X is similar to the normal Auger spectrum (Fig.2f),but the peaks are shifted to high energy. The peak X is ascribed to the participant Auger transition, and other peaks are attributed to the spectator Auger transition of the nitrogen 1s hole. The difference in spectra between Fig.1b and Fig.2b, which both correspond to resonant excitation to the π^*_{CN} orbital,

indicates that the spectator Auger transition depends on the site of core hole.

These results clearly show that primary excitation depends on the localized character of unoccupied orbital and the subsequent Auger transition depends on the site of core hole. The comparison of AEPICO measurements with the resonant Auger spectra at various resonant excitation supports the previous results, that the ion desorption depends on the bonding/anti-bonding character and the localized character of the excited state and the Auger final state [2, 3].

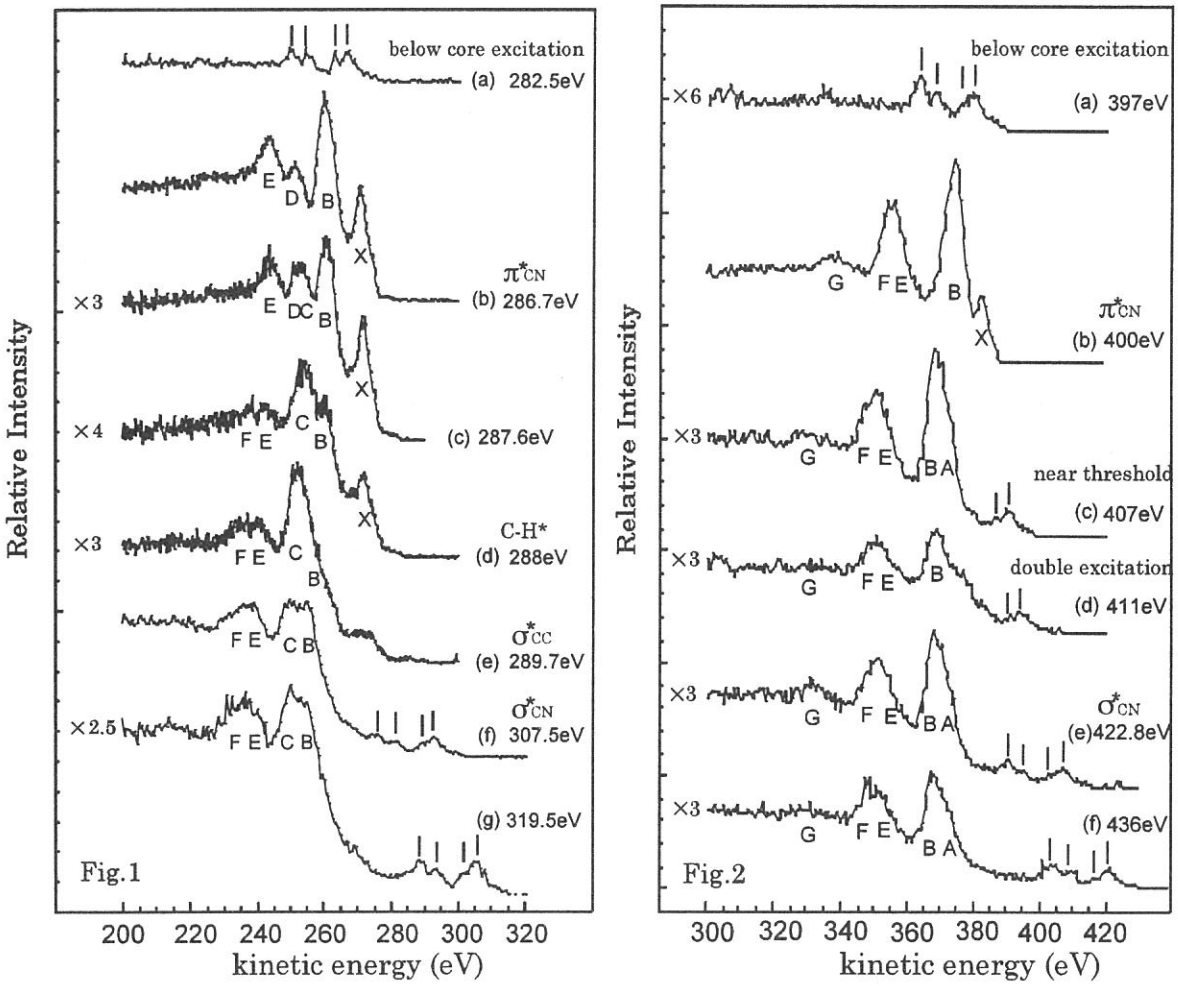

FIG.1 and FIG.2. Resonant Auger spectra for condensed CH_3CN following carbon core excitation (Fig.1), and nitrogen core excitation (Fig.2). Bars show peaks owing to emission of a valence electron. Photon energies are indicated at the right end.

Reference

[1] K. Mase et al., Rev. Sci. Instrum. 68 (1997) 1703.

[2] E. Ikenaga et al., UVSOR Activity Reports BL2B1. (1996) 108.

[3] T. Sekitani et al., Surf. Sci. 390 (1997) 107.

[4] J. V. Ortiz, J. Chem. Phys. 83 (1985) 4604.

[5] R. R. Rye and J. E. Houston, J. Chem. Phys. 75 (1981) 2085.

(BL2B1)

Site-specific fragmentation following C:1*s* core-level photoionization of CF_3CH_3 condensed on a Au surface

Shin-ichi Nagaoka, Kazuhiko Mase,[A] Mitsuru Nagasono,[A] Shin-ichiro Tanaka[A] and Tsuneo Urisu[A]

Department of Chemistry, Faculty of Science, Ehime University, Matsuyama 790-8577

[A]Institute for Molecular Science, Okazaki 444-8585

Synchrotron radiation has provided a powerful means to obtain information about core-level excitations, and the dynamic processes following the core-level excitations in molecules have long been a subject of interest. In contrast to valence electrons that are often delocalized over the entire molecule, the core electrons are localized near the atom of origin. Although core electrons do not participate in the chemical bonding, the energy of an atomic core-level in the molecule depends on the chemical environment around the atom. A shift in the energy levels of core electrons that is due to a specific chemical environment is called a chemical shift.

Monochromatized synchrotron radiation can excite core electrons of an atom in a specific chemical environment selectively, discriminating the core electrons from those of like atoms having different chemical environments. This site-specific excitation often results in site-specific fragmentation, which is of importance in understanding localization phenomena in chemical reactions and which is potentially useful for synthesizing materials through selective bond breaking.

To elucidate the site-specific fragmentation, we have studied the spectroscopy and dynamics following core-level photoionization of various molecules condensed on surfaces [1,2]. To observe the dissociation processes following core-level ionization of a site selectively, we use the energy-selected-photoelectron photoion coincidence (ESPEPICO) method and the Auger-electron photoion coincidence (AEPICO) method. The measurements of fragment ions coincidentally produced with energy-selected photoelectrons or Auger-electrons allow selective observation of the processes initiated by the electron ejection.

In the present work, we have used photoelectron spectroscopy and these coincidence methods to study the site-specific fragmentation following C:1*s* photoionization of CF_3CH_3 condensed on a Au surface. The chemical environment of a C atom bonded to three F atoms (C[F]) is very different from that of one bonded to three H atoms (C[H]), so it seems likely that CF_3CH_3 will show site-specific fragmentation. It is also interesting that the site-specific fragmentation pattern on a Au surface is compared with that in the vapor phase [3,4].

Since the accidental coincidences carried the time structure of the synchrotron source that was operated with a partial-filling mode, we had to remove the time-structure background with a period of 177 ns from the coincidence spectrum. Accordingly, we performed its fast-Fourier-transformation (FFT), subtracted the 177 ns component and then made its inverse FFT. This technique seems to work rather well such that we are able to discern even weak true coincidence

features rather well.

Figures 1(a) and 1(b) show the ESPEPICO spectra obtained with emission of the C[H]:1*s* and C[F]:1*s* electrons, respectively. $C_2H_n^+$ (n=0-3) and $CFCH_m^+$ (m=2,3) ions are predominantly desorbed coincidentally with the C[F]:1*s* electrons. The ionic fragmentation occurs selectively around the C atom where the photoionization has taken place: synchrotron radiation can indeed play the part of an optical knife for molecules. It is also interesting that the ratio of the coincidence count for CH_3^+ to that for CF_3^+ is larger in the case of C[H]:1*s* photoionization than in C[F]:1*s*. The site-specific fragmentation pattern obtained from excitation on the Au surface is very different from that obtained from excitation in the vapor phase [3,4].

Figure 2 shows the AEPICO spectrum obtained for the electron kinetic energy (E_k) corresponding to the C[H](*KVV*) normal-Auger transition. The AEPICO yield for CH_3^+ is greatly enhanced at the high-E_k edge of the C[H](*KVV*) normal-Auger peak. This result shows that the character of HOMO is C-C σ-bonding and the electronic transition from HOMO to C[H]:1*s* induces ionic fragmentation of the C-C bond.

[1] S. Nagaoka, K. Mase, M. Nagasono, S. Tanaka, T. Urisu and J. Ohshita, J. Chem. Phys., in press.

[2] S. Nagaoka, K. Mase and I. Koyano, Trends Chem. Phys., in press.

[3] K. Müller-Dethlefs, M. Sander, L. A. Chewter and E. W. Schlag, J. Phys. Chem. 88, 6098 (1984).

[4] W. Habenicht, H. Baiter, K. Müller-Dethlefs and E. W. Schlag, J. Phys. Chem. 95, 6774 (1991).

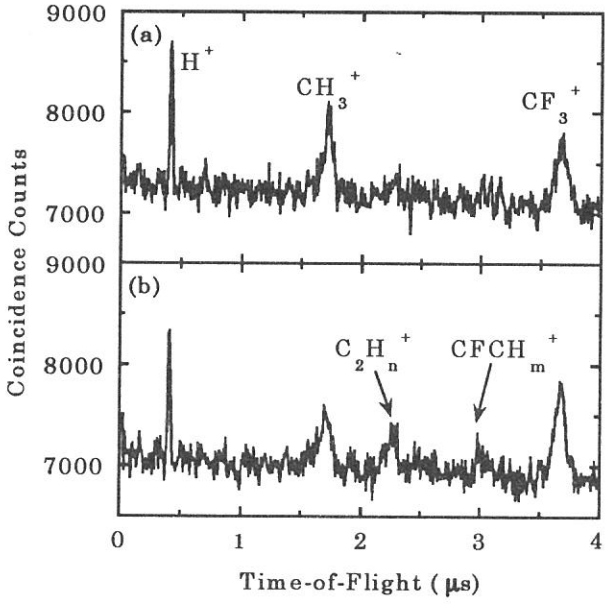

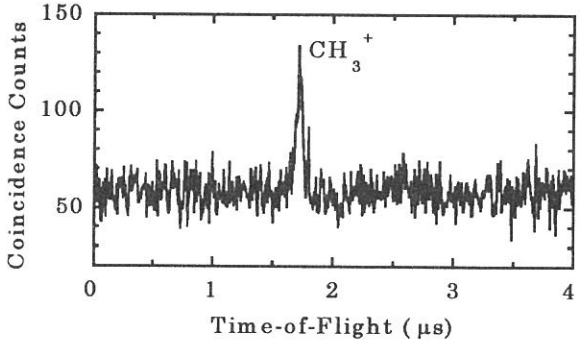

Figure 1 (left-hand side). ESPEPICO spectra of CF_3CH_3 taken at a photon energy of 393 eV. Data collection time is 5000 s. (a) C[H]:1*s* electron emission. (b) C[F]:1*s* electron emission.

Figure 2 (right-hand side). AEPICO spectrum obtained at a photon energy of 293 eV for E_k = 260 eV, which corresponds to the high E_k edge of the C[H](*KVV*) normal-Auger peak. Data collection time is 1080 s.

(BL2B1)

Site-specific fragmentation following Si:2*p* core-level photoionization of bridged trihalosilyl-trimethylsilyl system condensed on a Si(111) surface

Shin-ichi Nagaoka, Kazuhiko Mase,[A] Mitsuru Nagasono,[A] Shin-ichiro Tanaka[A] and Tsuneo Urisu[A]

Department of Chemistry, Faculty of Science, Ehime University, Matsuyama 790-8577

[A]Institute for Molecular Science, Okazaki 444-8585

In a previous paper [1], we used photoelectron spectroscopy and the energy-selected-photoelectron photoion coincidence (ESPEPICO) method to study site-specific fragmentation following Si:2*p* photoionization of 1-trifluorosilyl-2-trimethylsilylethane [$F_3SiCH_2CH_2Si(CH_3)_3$, FSMSE] condensed on a Au surface. The photoelectron spectrum of FSMSE had two peaks for 2*p*-electron emission: one for the Si atom bonded to three methyl groups (Si[Me]) and one for the Si atom bonded to three F atoms (Si[F]). H^+ and F^+ ions were predominantly desorbed coincidentally with the Si[Me]:2*p* and Si[F]:2*p* electrons.

The site-specific fragmentation is potentially useful for synthesizing materials through selective bond breaking. Synchrotron radiation can indeed play the part of an optical knife for molecules. When bond dissociation around an atomic site is required in the synthesis, one can use the optical knife that has the photon energy corresponding to the specific excitation of that site. In this context, the dependence of the site-specific fragmentation on the distance between the sites is interesting [2]. How far must the atomic site of interest be separated from any other atomic site around which bond dissociation is undesirable, in order for the site-specific process to work? This point is closely related to the application to the construction of future molecular electric devices, in which the control of very localized reactions will play a crucial role. Accordingly, in the present study, we have studied the site-specific fragmentation following Si:2*p* photoionization of 1,1,1-trimethyltrichlorodisilane [$Cl_3SiSi(CH_3)_3$, MCDS], 1-trifluorosilyl-2-trimethylsilylmethane [$F_3SiCH_2Si(CH_3)_3$, FSMSM] and FSMSE condensed on a Si(111) surface. The measurements of fragment ions coincidentally produced with energy-selected photoelectrons allow selective observation of the processes initiated by the electron ejection.

Figures 1(a), 1(b) and 1(c) show the total electron yield (TEY) spectrum of MCDS, FSMSM and FSMSE condensed on Si(111), respectively. Assignments of peaks in the spectra, inferred by comparison with the photoabsorption spectra of $SiCl_4$, SiF_4 and $Si(CH_3)_4$, are given in the figure. The TEY spectra of FSMSM and FSMSE are made up of the superposition of those of $Si(CH_3)_4$ and SiF_4, but that of MCDS seems to be close to that of $Si(CH_3)_4$. These results show that the site-specific excitation occurs in FSMSM and FSMSE but it does not in MCDS.

Figures 2(a), 2(b) and 2(c) respectively show the photoelectron spectra of MCDS, FSMSM and FSMSE in the region of Si:2*p* electron emission. The photoelectron spectra of FSMSM and FSMSE have two peaks in this region. The peaks at the lower- and higher-energy sides are respectively thought to correspond to Si[Me]:2*p* and Si[F]:2*p* electron emissions. However, under

the same experimental conditions, the photoelectron spectrum of MCDS has only one peak.

Figures 2(a), 2(b) and 2(c) also show the ESPEPICO yield spectra in MCDS, FSMSM and FSMSE respectively in the region of Si:2*p* electron emission. In FSMSM and FSMSE, the ESPEPICO yield for H^+ shows a peak around the binding energy of Si[Me]:2*p*, and the yield for F^+ shows a peak around that of Si[F]:2*p*, although the peak for F^+ is less remarkable in FSMSM than in FSMSE. However, H^+ is the only primary species desorbed coincidentally with the Si:2*p* electron in MCDS. These results show that the site-specific fragmentation takes place in FSMSM and FSMSE but it does not in MCDS.

From the above-mentioned results, it is considered that the site-specific excitation and fragmentation are observed in molecule in which the two Si sites are located far from each other. This is because the electron-migration between the two Si-containing groups located far from each other (for example, F_3Si- and -$Si(CH_3)_3$ in FSMSE) is not effective, as described previously [2].

[1] S. Nagaoka, K. Mase, M. Nagasono, S. Tanaka, T. Urisu and J. Ohshita, J. Chem. Phys., in press.

[2] S. Nagaoka, T. Fujibuchi, J. Ohshita, M. Ishikawa and I. Koyano, Int. J. Mass Spectrom. Ion Processes, in press.

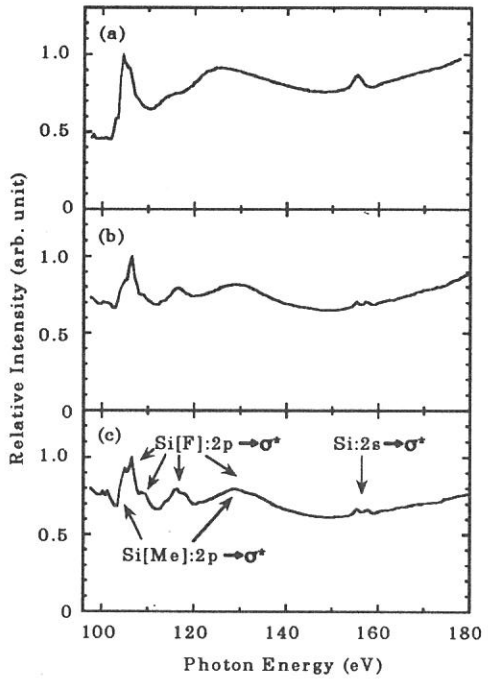

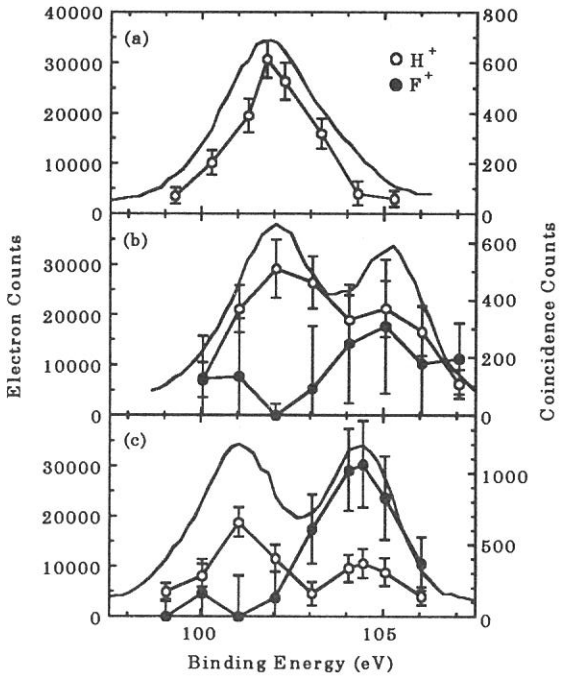

Figure 1 (left-hand side). TEY spectrum. (a) MCDS. (b) FSMSM. (c) FSMSE. Each channel was measured for 2 s at a step of 0.5 eV.

Figure 2 (right-hand side). ESPEPICO yield spectra and the photoelectron spectrum as a function of electron binding energy in the region of Si:2*p* electron emission. Each channel in the photoelectron spectrum was measured for 0.5 s at a step of 0.2 eV. (a) MCDS. Data collection time for each data point in an ESPEPICO yield spectrum is 1800 s. (b) FSMSM. Data collection time is 1200 s. (c) FSMSE. Data collection time is 1320 s.

(BL2B1)

Study of ion desorption induced by resonant core–electron excitations of condensed methanol using Auger electron photoion coincidence (AEPICO) spectroscopy combined with synchrotron radiation

Kazuhiko Mase, Mitsuru Nagasono, Shin–ichiro Tanaka, and Tsuneo Urisu

Institute for Molecular Science, Okazaki 444–8585, Japan

Ion desorption induced by resonant core–electron excitations of molecules condensed on a surface is a prospective topic in molecular dynamics, surface science, and synchrotron radiation researches [1]. Auger electron photoion coincidence (AEPICO) spectroscopy is an ideal tool in this field, because it provides ion desorption yield derived from the selected Auger transitions [2]. In the present article, we describe an ion desorption study in the region of resonant excitations of Carbon 1*s* core–electron of condensed methanol using total ion and Auger electron yield spectroscopy (TIYS and AEYS), non–derivative Auger electron spectroscopy (AES), and AEPICO spectroscopy. Figure 1(a) shows TIYS of condensed CH_3OD, CH_3OH, and CD_3OH in the Carbon K–edge region. Since the desorption probability of D^+ and polyatomic ions such as CH_3^+ is much smaller than that of H^+, the total ion yield corresponds to the H^+ yield [3]. CH_3OD and CH_3OH exhibited TIYS which resemble to each other, while ions are scarcely desorbed from CD_3OH. This result shows that H^+ desorption from the hydroxyl group is suppressed as compared with that from the methyl group, which is in consistent with the results of an electron–stimulated desorption study of condensed methanol [3]. We ascribed this phenomenon to the hydrogen bonding due to the trimer and dimer formation [4] on the surface. The AEYS exhibited a peak at $h\nu$ = 287.8 eV and a broad peak around $h\nu$ = 292.3 eV. The spectrum of TIY/AEY, on the other hand, exhibited a small peak at $h\nu$ = 287.8 eV and a slight suppression at $h\nu$ = 292.3 eV. Therefore we assigned $h\nu$ = 287.3 eV to the resonance into weakly C–H anti–bonding orbital (C–H*), $h\nu$ = 292.8 eV to the resonance into C–H non–bonding orbital, and $h\nu$ = 292.8 eV to C:1*s* ionization, respectively. Figure 2 shows series of AEPICO spectra at $h\nu$ = 287.8, 292.3, and 315.3 eV for the electron kinetic energies of 220–275 eV corresponding to the C:KVV Auger transitions. H^+ was found to be the only ion species desorbed in all the cases. Figure 3 shows the electron kinetic energy dependence of the AEPICO yield (AEPICO yield spectra) at $h\nu$ = 287.8, 292.3, and 315.3 eV. The valence electronic configuration of CH_3OH is $(3a')^2(4a')^2(5a')^2(1a'')^2(6a')^2(7a')^2(2a'')^2$ [5]. At $h\nu$ = 315.3 eV, the AEPICO yield spectrum exhibited the maximal peak at the electron kinetic energy of 255 eV, which corresponds to $(1a'')^{-2}$, $(1a'')^{-1}(6a')^{-1}$, and $(6a')^{-2}$ Auger final states [6], where 1a" and 6a' are the C–H bonding orbital [5]. This result indicates that the normal–Auger stimulated ion desorption (normal–ASID) mechanism is responsible at $h\nu$ = 315.3 eV. At $h\nu$ = 287.8 eV, the AEPICO yield spectrum exhibited a peak at the electron kinetic energy of

260 eV which was assigned to $(1a'')^{-2}(C\text{-}H^*)^1$, $(1a'')^{-1}(6a')^{-1}(C\text{-}H^*)^1$, and $(6a')^{-2}(C\text{-}H^*)^1$ spectator–Auger final states. This result suggests that spectator–ASID mechanism and/or ultrafast ion desorption mechanism is predominant at $h\nu$ = 287.8 eV. At $h\nu$ = 292.3 eV, on the other hand, the AEPICO yield spectrum displayed a remarkable suppression at the electron kinetic energy of 260 eV in contrast to the case at $h\nu$ = 287.8 eV. This suppression was ascribed to the reduction of the hole–hole Coulomb repulsion due to the shield effect of the electron in the non-bonding orbital. This result suggests that spectator–ASID mechanism is probable at $h\nu$ = 292.3 eV.

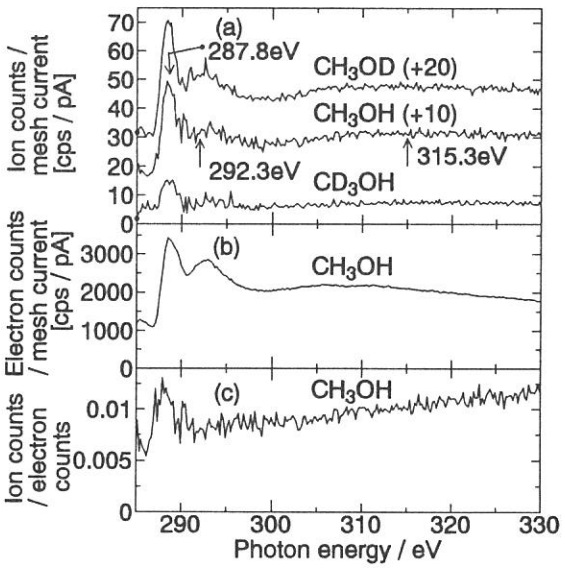

Figure 1. (a) TIYS of condensed CH_3OD, CH_3OH, and CD_3OH. (b) AEYS, and (c) spectrum of TIY/AEY of condensed CH_3OH.

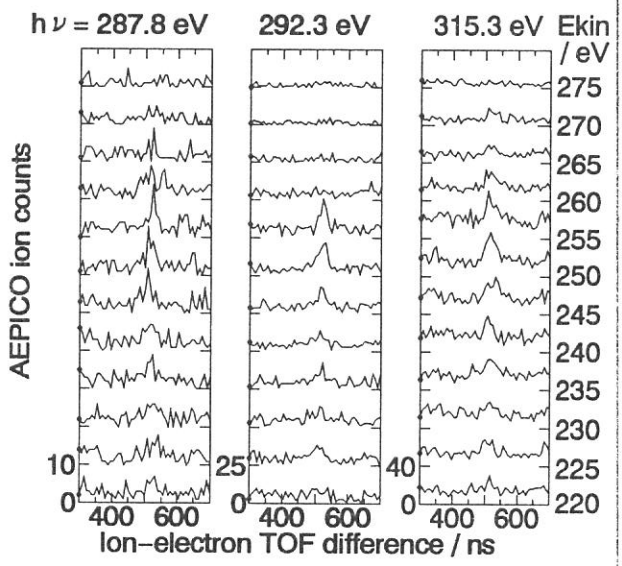

Figure 2. Series of AEPICO spectra at $h\nu$ = 287.8, 292.3, and 315.3 eV.

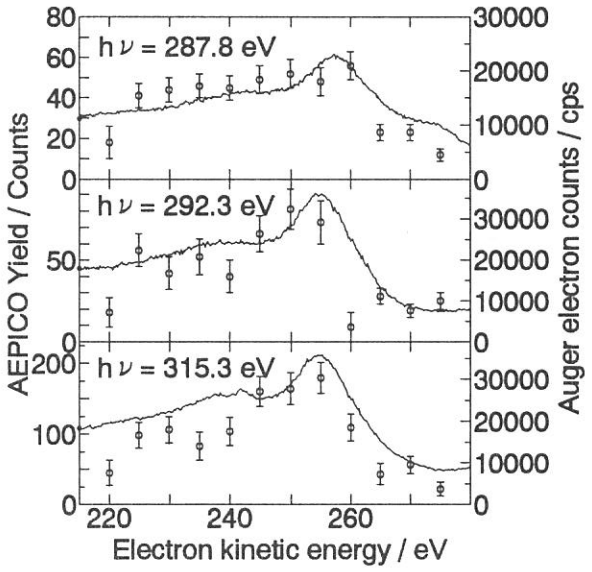

Figure 3. (a) AEPICO H^+ signal intensities as a function of the electron kinetic energy (AEPICO yield spectra) at $h\nu$ = 287.8, 292.3, and 315.3 eV. The solid lines show the AES.

References

[1] K. Mase *et al.*, *Surf. Sci.* **390**, 97 (1997); M. Nagasono *et al.*, *Surf. Sci.* **390**, 102 (1997); T. Sekitani *et al.*, *Surf. Sci.* **390**, 107 (1997).

[2] K. Mase *et al.*, *Rev. Sci. Inst.* **68**, 1703 (1997).

[3] R. Stockbauer *et al.*, *J. Chem. Phys.* **76**, 5639 (1982).

[4] O. Mó *et al.*, *J. Mol. Struct. (Theochem)* **314**, 73 (1994).

[5] M. B. Robin and N. A. Kuebler, *J. Electron Spectros. Relat. Phenom.* **1**, 13 (1972/73).

[6] N. Kosugi, Master's thesis (1978).

(BL3A1) Fine Processing of PMMA with Synchroton Radiation

Akitaka Yoshigoe, Takanori Hayakawa, Hitoshi Sato, Akihiro Wakahara and Akira Yoshida

Department of Electrical and Electronic Engineering, Toyohashi University of Technology, Tenpaku-cho, Toyohashi, 441, Japan

Recently, semiconductor devices on a small Si chip have been remarkably integrated. The lithography technology generally accepted at present can't follow this development. Therefore, the superior dry processing using vacuum-ultra-violet light is required in the future. In this study, we have demonstrated that PMMA (polymethyl-methacrylate) films, which are widely used as an electron beam and X-ray positive resist, were irradiated by SR in vacuum and oxygen gas.

The PMMA was spin coated on the Si wafer with a few micrometer thick. The sample was introduced into the high vacuum reaction chamber. The exposure to undulator light (undulator gap: 60mm) was performed directly through differential pumping systems. Figure 1 shows the reduced thickness of PMMA films which is normalized by the initial thickness as a function of SR exposure doses with and without the oxygen gas. The substrate temperature was room temperature during the SR irradiation. It was found that the reduced thickness increased with increasing the SR exposure dose at the low SR exposure and then it was saturated. On the other hand, it was found that the PMMA films were etched and removed with oxygen gas during SR irradiation.

Figure 2 shows the XPS (X-ray photoelectron spectroscopy) spectra of PMMA films and the samples after SR irradiation with and without oxygen gas. It should be pointed out that Si2p signals of the substrate were observed when the oxygen gas exists during the SR irradiation. No Si signals, however, were observed in the case of vacuum.

From the results of the XPS and the thickness measurements, it was found that the PMMA films were not etched up to the Si substrate in vacuum, however, completely removed to the substrate surface in oxygen gas.

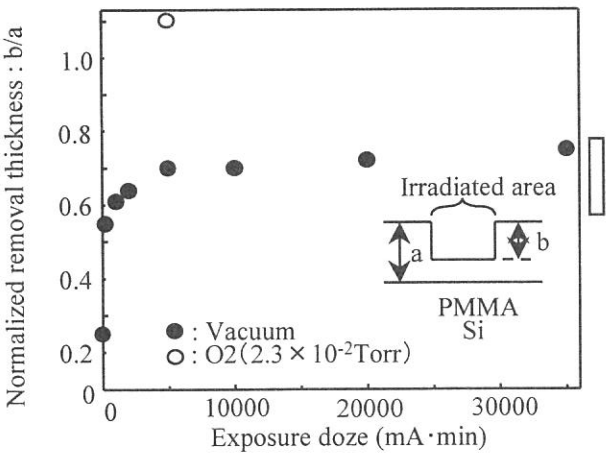

Fig. 1. The reduced thickness of PMMA after SR irradiation in vacuum and oxygen gas.

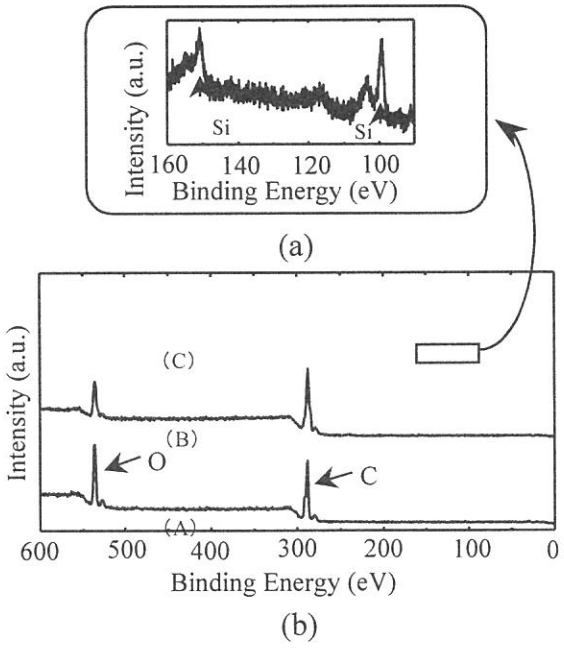

Fig. 2. XPS spectra. (A) PMMA, (B)SR irradiation in vacuum, (C) in oxgen gas.

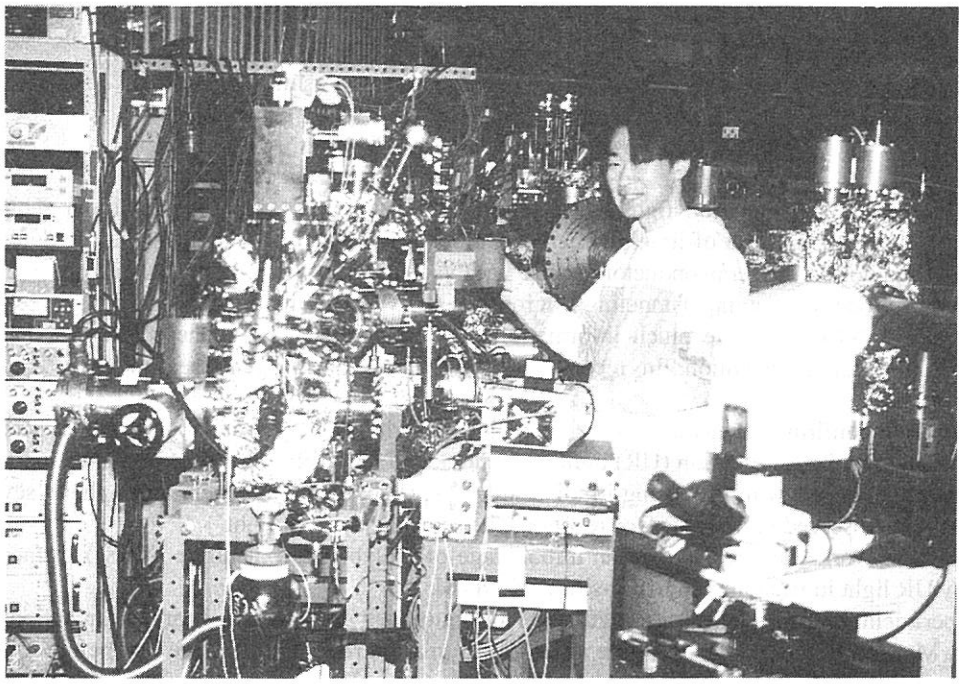

Photoreaction Chamber at BL8A

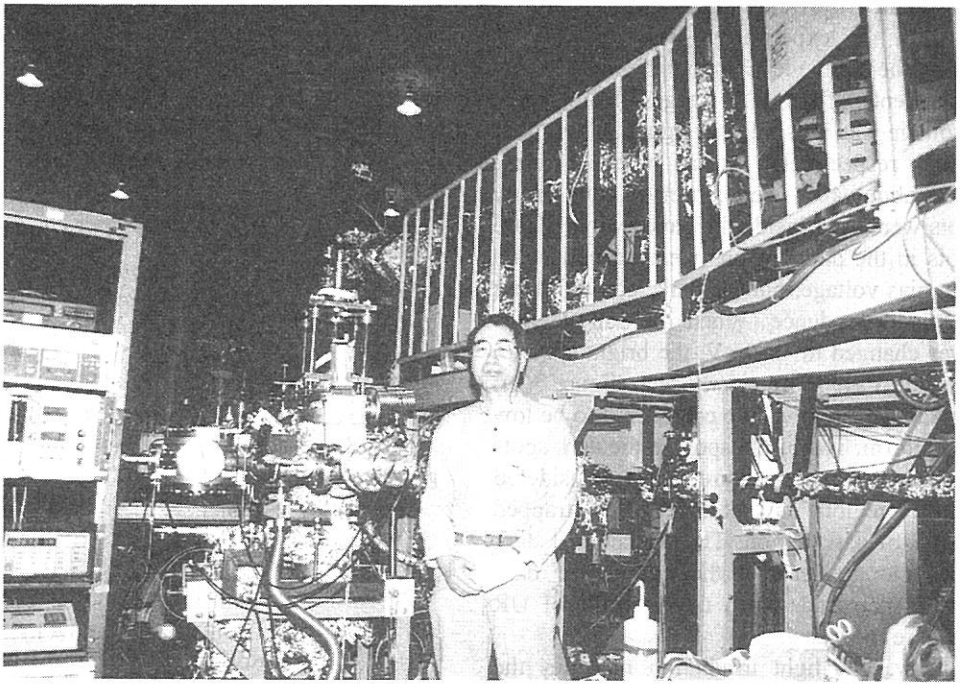

Prof. Murata (Univ. of Kyoto Edu.) at BL7A and BL7B

(BL3A-1)

Observation of MoS_2 surface reaction irradiated by Undulator Radiation Light Using Scanning Tunneling Microscope

T.Hayakawa, A.Yoshigoe and A.Yoshida

Toyohashi University of Technology, Toyohashi 441-8580

Recently, synchrotron radiation light has been exploited to give a new possibility in semiconductor processing technology because of its high energy photons. Investigations to understand the defect creation and atomic behavior on the semiconductor surface with vacuum ultra-violet-light give important clues to the semiconductor process. Scanning Tunneling Microscope (STM) is a direct method working in real space on an atomic scale. STM can give much information of electronic states and the surface topography with extremely high spatial resolution. In recent years, STM has been often used to analyze the surface characterization.

Last year, we confirmed that the depression region and ring pattern were found on the MoS_2 surface irradiated with Undulator Radiation (UR) light in vacuum, and these patterns became greater and the number of the patterns increased with increasing irradiation UR light dose. In the oxygen atmosphere, several kinds of patterns were observed in these surface reactions the same dose of UR light.

In the present work, we have studied an initial stage of molybdenum disulfide (MoS_2) surface reactions induced by UR light in vacuum with an in-situ UHV-STM.

The experimental set-up is shown in Figure 1. This equipment consists of preparation, reaction, and STM chambers. MoS_2 was used as the substrate and cleaved in air at room temperature just before it was loaded into the preparation chamber. The sample was transferred into the reaction chamber under a base pressure below 1×10^{-7} Torr and irradiated by UR light at room temperature. The amount of UR light dose was 25mA·min, 100mA·min, 200mA·min and 300mA·min. After the irradiation, the sample was transferred to the UHV-STM chamber and the surface topography was observed. STM images were obtained both in the constant-height mode and the constant-current mode at the sample bias voltage in the range of -500mV～500mV.

Figure 2(a) shows the STM image of MoS_2 clean surface on 60Å×60Å scale with the sample bias voltage of -150mV and the tunneling current of 1nA. The atomic structure in the top layer of sulfur atoms was seen clearly. Figure 2(b) shows the cross section of STM image of MoS_2 clean surface. The lattice constant estimated from this figure is consistent with that calculated from X-ray diffraction pattern of this sample within the experimental error of 2%. The images obtained with this STM are reasonable. Furthermore, the atomic level image of graphite sample was observed.

The dependence of the STM images of MoS_2 surface irradiated by UR light for 25mA·min in vacuum on the bias voltage was illustrated in figure 3. The sample bias voltages in figure 3(a) and 3(b) are both 150mV and -150mV, respectively. As can be seen from figure 3(a), the dark circular regions with an average diameter of about 40Å were observed, and many bright spots were seen inside the dark region. These bright spots in the dark regions were dependent on the sample bias voltage, but the dark region did not show such a dependence. When the sample bias voltage was changed to -150mV, the bright spots in the dark region were more clearly seen.(figure 3(b)) Therefore, the dark regions are considered to be low area at a landform. The bright spots in the dark spots are due to the electronic structure, so it is considered that some dark regions have some electrons trapped on the center of dark region. The diameter of dark regions became greater and the number of dark regions were increased, when the amounts of UR light dose were increased.

In summary, UR light irradiation modifies the MoS_2 surface, and the modified surface structure has been made clear on a atomic scale with STM.

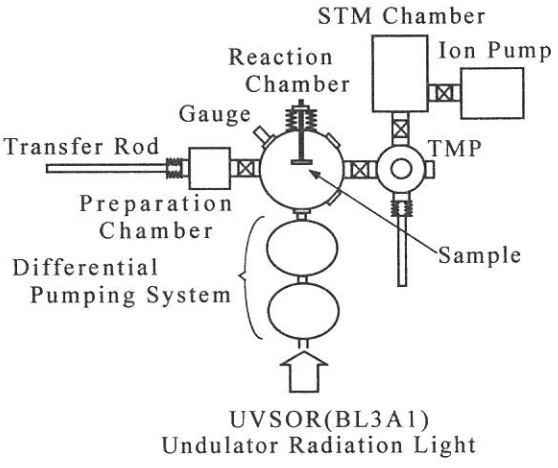

Fig.1 Experimental set-up

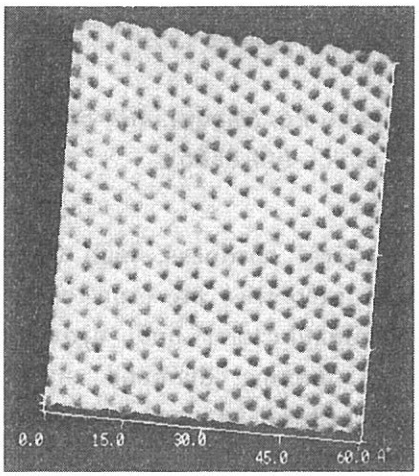

(a) STM image of the MoS_2 clean surface (60 Å × 60 Å)

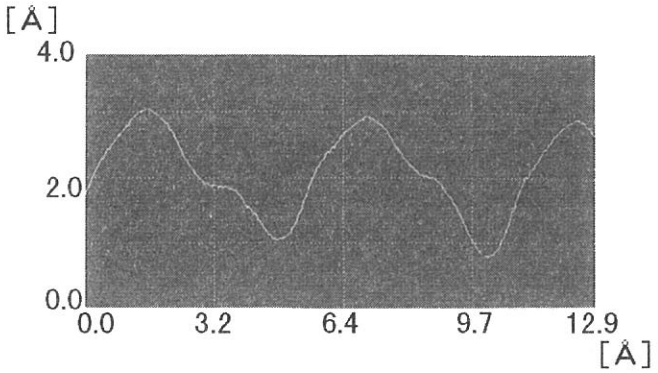

(b) Cross section of STM image of the MoS_2 clean surface

Fig.2 MoS_2 clean surface

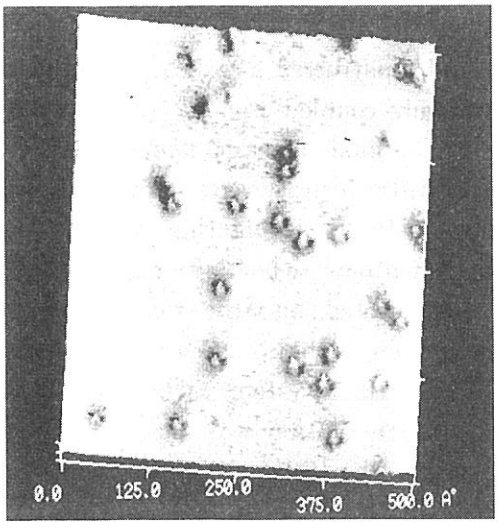

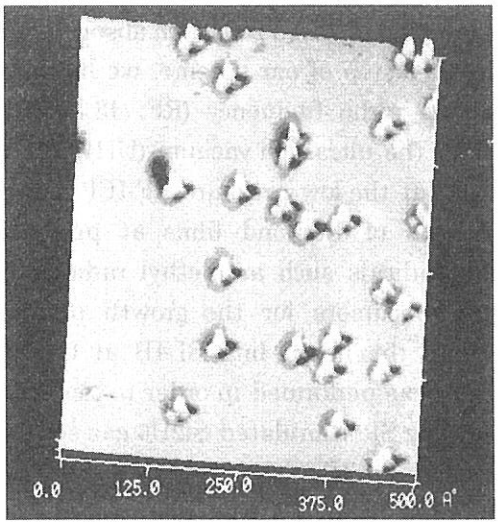

(a) Sample bias voltage 150mV (500 Å × 500 Å)

(b) Sample bias voltage -150mV (500 Å × 500 Å)

Fig.3 STM images of the MoS_2 irradiated for 25mA·min in vacuum

(BL4B)

Investigation of diamond growth mechanism using infrared reflection absorption spectroscopy

Mineo Hiramatsu, Hideyuki Noda, Masahito Nawata and Tsuneo Urisu[A]

Faculty of Science and Technology, Meijo University, Tempaku-ku, Nagoya, 468-8502
[A]Institute for Molecular Science, Myodaiji, Okazaki, 444-8585

Diamond has many excellent properties, including mechanical hardness, high thermal conductivity, chemical inertness, and a wide band gap. These properties are expected to be applied to mechanical cutting tools, heat sinks of semiconductors, and high-energy light-emitting materials. Therefore, various techniques of forming diamond such as plasma-enhanced chemical vapor deposition and hot-filament chemical vapor deposition have been developed. For the application of diamond film to the electronic devices in nanometer scale, area-selective growth of diamond must be one of key technologies for the formation of diamond films in extremely fine pattern. To accomplish this object, synchrotron radiation (SR) is expected to be useful because it provides a high spatial resolution with high photon energy.

In the present work, we are planning to deposit diamond film area-selectively using radical injection technique[1,2] with the assistance of SR-induced chemical reaction. For this purpose, first of all, it is necessary to make clear of diamond growth mechanism on the substrate. Our primary goal is to investigate the surface reaction of diamond growth in the early stage of deposition using infrared reflection absorption spectroscopy (IRAS).

As the first step of our scheme, we have designed and constructed a radical source using a low pressure radio frequency (RF; 13.56 MHz) inductively coupled plasma (ICP), which is specified for the ultrahigh vacuum (UHV) equipment. By the basic research using ICPs, it was confirmed that the low pressure RF-ICP using methanol-water-hydrogen system was useful for the formation of diamond films at pressures below 15 Pa[3]. Using this radical source, important radicals such as methyl radicals and hydrogen atoms, which are regarded as the important precursors for the growth of diamond, are injected into the reaction chamber connected to the beam line BL4B at UVSOR, Institute for Molecular Science. Preliminary experiment was performed in order to confirm the validity of IRAS system. SiHx on the Si (100) surface during SR-stimulated Si2H6 gas source molecular beam epitaxy was detected by means of IRAS using a CoSi2 buried metal layer (BML) substrate. The IRAS system installed to the UHV chamber at BL4B was re-arranged for the observation of the surface reaction on the substrate under irradiation of SR beam and injection of radicals. The detection of CHx is being carried out using BML and metal (copper and platinum) substrates.

[1] M. Hiramatsu, M. Inayoshi, K. Yamada, E. Mizuno, M. Nawata, M. Ikeda, M. Hori, and T. Goto, Rev. Sci. Instrum., 67 (1996) 2360.

[2] M. Ikeda, E. Mizuno, M. Hori, T. Goto, K. Yamada, M. Hiramatsu, and M. Nawata, Jpn. J. Appl. Phys., 35 (1996) 4826.

[3] H. Noda, M. Hiramatsu, M. Nawata, M. Hori, and T. Goto, Bulletin Am. Phys. Soc., 42 (1997) 1753.

(BL4B)

Quantum Dot Formation Using Synchrotron Radiation-excited Etching

Youichi Nonogaki[a], Tsuneo Urisu[a] and Yoshikazu Takeda[b]

[a]*Institute for Molecular Science, Myodaiji, Okazaki 444-8585, Japan*
[b]*Department of Materials Science and Engineering, Graduate School of Engineering, Nagoya University, Furo-cho, Chikusa-ku, Nagoya 464-8603, Japan*

Semiconductor structures with reduced dimensionality are subject of significant interest in modern solid state physics and device application. Recently the formation of quantum-sized InAs and InGaAs dots self-organized on GaAs surfaces using molecular beam epitaxy (MBE) was demonstrated[1]. We have been studying formation of InAs dots on InP substrate by novel droplet heteroepitaxy[2,3], because the quantum dots can emit light at technologically important wavelength of 1.5 μm. Although emission from the single dot has very sharp line, the total emission from the sample has broad peak of which full width at half maximum is about 100-150 meV, probably due to size fluctuation between each dot. Suppression of the fluctuation to sharpen the emission is necessary to fabricate the new optical devices which have higher performance than quantum laser diodes.

We suggested a new method to form ordered array of the quantum dots which includes synchrotron radiation (SR) -excited etching process. The SR-excited etching process has great potentials for fabrication of semiconductor devices. The etching reaction occurs only at SR irradiated area, then the etching progresses straight with no lateral etching. Furthermore, damage induced by SR-excited etching is much lower than commonly used reactive ion etching, because SR-excited etching involves no sputter process.

Figure 1 (a) and (b) show schematic illustrations of our proposal to form the ordered array of the quantum dots. The SR-excited etching process is performed as shown in Fig. 1 (a), where SiO_2 on InP substrate is exposed to SR in SF_6 and O_2 ambient. Therefore, SiO_2 is patterned by masking of Al_2O_3 plate with ordered holes. After preparation of patterned substrate, InAs or InGaAs quantum dots are formed by selective growth technique using organometallic vapor phase epitaxy (OMVPE), as shown in Fig. 1 (b).

We are now improving and reconstructing of etching chamber and differential pumping system to start SR-excited etching experiments.

References

[1]D. Leonard, K. Pond and P.M. Petroff, Phys. Rev. B **50**, (1994) 11687.
[2]Y. Nonogaki, Y. Fujiwara, Y. Takeda et al., Appl. Surf. Sci. **117/118**, (1997) 665.
[3]Y. Nonogaki, Y. Fujiwara, Y. Takeda et al., Mat. Sci. & Eng. B (in press).

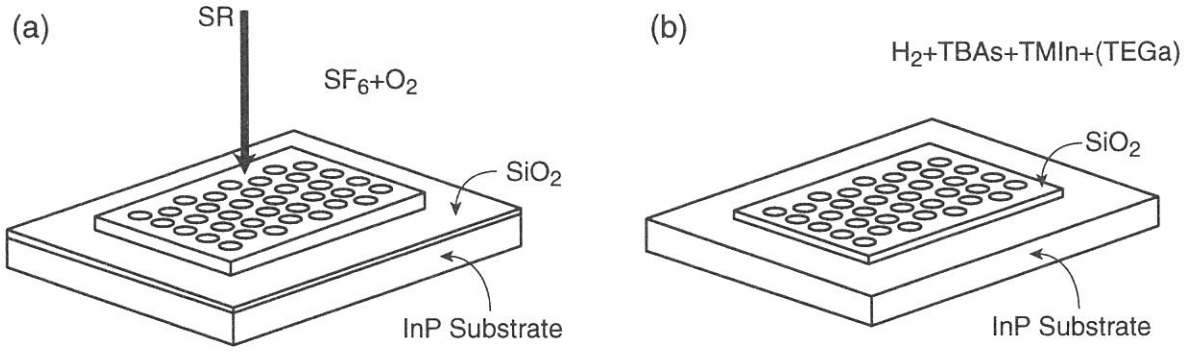

Fig. 1. Schematic illustrations of (a) the SR eching process and (b) subsequent selective growth process to form ordered array of the quantum dots.

(BL5A) **Interpretation of the photoelectron spectrum of H_2O/Si(100) surface**

Shin-ichiro Tanaka, Junichi Murakami and Masao Kamada

Institute for Molecular Science, Okazaki, 444-8585, Japan

The adsorbed states of water on the Si surface has been studied by many experimental methods, because not only it is important process of the wet oxidation of the Si, but also it is one the model case of the adsorption of the molecule on the semiconductor surface. Schmeisser et.al. [1] studied this system by the use of the photoelectron spectroscopy, and concluded the adsorption in the molecular form. Meanwhile, Ibach et.al. [2] and Nishijima et.al.[3] used HREELS (High-resolution electron energy loss spectroscopy) and concluded that water is dissociated into OH and H on the Si surfaces. Chabal et.al. [4] also stated the dissociative adsorption by the use of the infrared spectroscopy. It is considered that the vibrational spectroscopy is supreme to the photoelectron spectroscopy in order to determine the bonding configuration of the surface, and thus, the dissociative adsorption is generally accepted for this system. However, it means that the results of the photoelectron spectroscopy should be re-interpreted, but the situation is rather contradictory. Ciraci et.al. [5] made a theoretical calculations and stated that the photoelectron spectrum can be interpreted according to their model, however, their results is not agreement with the experimental results by the use of the synchrotron radiation as shown below. Schmeisser et.al. [6] made an *in-situ* experiments by using the HREELS and photoelectron spectroscopy and concluded that the water dissociation occur due to the electron beam of HREELS, however, it is not consistent with the results by Chabal et. al. [4], and can be denied.

Figure 1 shows the photoelectron spectroscopy of the Si(100) surface, which was cleaned by the resistive heating, exposed to 5L of water at the room temperature. Measurements were made by the SGM-TRAIN monochromator and Omicron EA-125HR analyzer installed at the BL5A of UVSOR. The photon energy was 52 eV, and the total resolution including photons and electrons was about 0.15eV. The angle of the incident photon and the detection of the electron was 45° and 0° from the surface normal. Energy positions (shifted by 2.2 eV to cancel the reference level difference) of peaks observed in the photoelectron spectrum of gaseous water and their assignments are also shown together with energy positions of calculated DOS (density of states) for the Si-OH and Si-H surface species. In the assignments of the calculation, "2σ" and "3σ" indicate the MOs (molecular orbital) of mainly the O-H bond, "O-σ" indicates the MO of mainly the Si-O bond, "O-π" indicates the lone pair of the O atom, and "H" indicates the MO of the Si-H bond. The calculation for upper one was made by Ciraci et.al.[5], and the lower one was made by Katircioglu [7]. Obviously, the calculations seems not to be agreement not only each other but also with the experimental results even if they are shifted by a constant energy to compensate the uncertainty of energy reference, and the interpretation can not be made by comparison to the calculation. Previously, Ciraci et. al. [5]. and Oellig et. al. [8]. made an assignments as the peak B to "H" and C

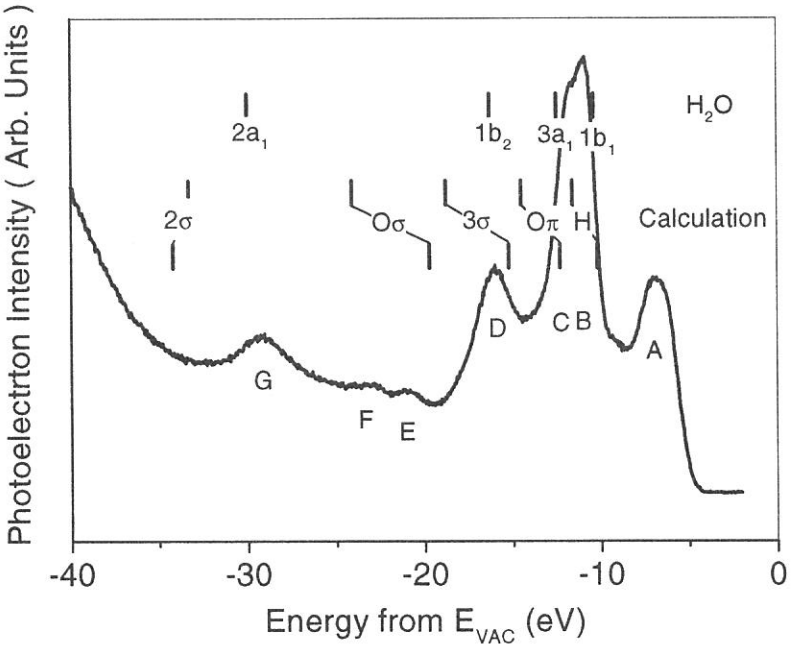

Figure 1

to "O-π". However, Schmeisser claimed that, based upon the comparison with their photoelectron spectroscopic study of the Si surface exposed to the atomic hydrogen, the peak B could not be ascribed to the Si-H species because the intensity was too high, and because the decrease taken at the higher photon energies, which was observed for the Si-H system, was not observed. It seems that the emission due to the Si-H species may be hidden in the peak A. Larsson et.al.[9] assigned both of the peaks B and C to "O-σ", which was divided to two components because the Si-O bond axis is tilted from the surface normal. However, their assignment does not agree the experimental results below, and can be denied.

We measured the photon energy dependence of the photoelectron spectra in order to get an information of the origin of the peaks in the spectrum (figure 2). The intensities of peak C (indicated in fig.1) are obviously changed depending upon photon energies. The intensity of the peak C is smaller than that of the peak B in the spectrum taken at hν=52 eV, however, it is larger taken at around 27 eV. According to the spectrum taken by the use of the He-discharge lamp, the peak C is smaller, again, taken at hν=22eV. Thus, it seems that the peak C resonantly enhances in intensity for the photon energy of around 30 eV, and that the origin of the peaks B and C are of different characters, which is inconsistent with the assignments by Larsson et.al. The resonance enhancement of the photoelectron peaks at photon energy of around 30 eV was observed for the "4σ" photoelectron peak of the carbon monoxide chemisorbed on metal surfaces [10]. It is ascribed to the "σ resonance", that is the enhancement of the photoelectron emission intensity of the molecular orbital with σ symmetry when the excitation energy corresponds to the transition to the σ* quasi-bound state. In the spectrum of the OH on the Si(100) surface, similar resonance may be expected, and the peak C may be interpreted to the molecular orbital with σ symmetry, thus, to "3σ" molecular orbital. Other peaks are assigned as follows. The peak B is assigned to "O-π". Based on the Schmeiser's discussion, the molecular orbital of Si-H bond is considered to be hidden in the peak A. The peak A also contain the contribution of the emission from the valence band of the Si substrate. The peaks D and G are assigned to "O-σ" and "2s", respectively. The peaks E and F have not reported until this report. The intensity is small, and may not be assigned to the single electron excitation from any particular molecular orbital, but satellite due to the multi-electron excitation and/or energy loss peaks of the peaks B-D due to the surface plasmon.

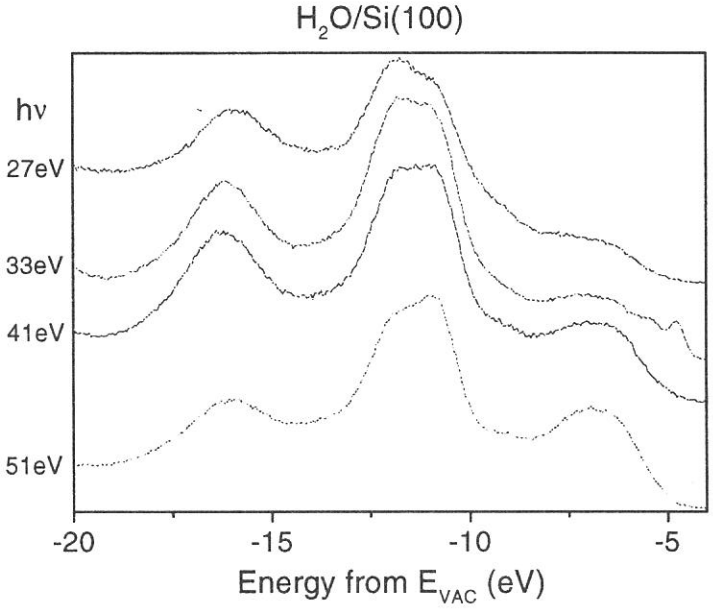

Figure 2

[1] D. Schmeisser et.al., Phys. Rev. B27, 7813(1983).
[2] H. Ibach et.al., Solid State Commun. 42, 457(1982).
[3] M. Nishijima et.al., J. Chem. Phys. 84, 6458(1986).
[4] Y. J. Chabal et.al., Phys. Rev. B29, 6974(1984).
[5] S. Ciraci et.al., Phys. Rev. B27, 5180(1983).
[6] D. Schmeisser et.al., Phys. Rev. B33, 4223 (1986).
[7] S. Katircioglu, Surf. Sci. 187, 569(1987).
[8] E. M. Oellig et.al., Solid State Commun. 51, 7(1984).
[9] C. U. S. Larsson et.al., Vacuum 42, 297(1991).
[10] F. Greuter et.al., Phys. Rev. B27, 7117(1983).

(BL5B)

Photon stimulated desorption of excited dimer from the surface of solid Ne by exciton creation

T. Hirayama*, T. Adachi, A. Hayama, I. Arakawa, K. Mitsuke[A] and M. Sakurai[A]

Department of Physics, Gakushuin University, 1-5-1 Mejiro, Toshimaku, Tokyo 171-8588
[A]*Institute for Molecular Science, Myodaiji, Okazaki 444-8585*

We have been studying the desorption of excited particles from the surface of rare gas solids (RGSs) induced by exciton creation using photon- and electron- stimulated desorption (PSD and ESD) techniques.[1-3] As to the excited atom desorption, two mechanisms, excimer dissociation (ED) and cavity ejection (CE), have been proposed[4] and confirmed experimentally. ED process is similar to the dissociation of an excited dimer (excimer) in the gas phase, i.e., the energetic fragment desorbs from the surface by the dissociation of a molecular-type exciton. Negative electron affinity of the matrix is known to be essential for the CE process to have a repulsive interaction between the excited atom and the surrounding ground state atoms, so that desorbed atoms via the CE mechanism are essentially in excited states. The desorption via CE mechanism can be observed only for solid Ne and Ar, but not for solid Kr and Xe because of their positive electron affinities in the bulk, while ED process is known to occurs for all rare gas solids.

Desorption of an excimer from the surface of RGSs has been predicted theoretically for solid Ne[5], Ar[6], and Kr[7], but the experimental evidence has been obtained only for solid Ar[8]. We have previously observed the emission from the desorbed particles with long lifetime from the surface of solid Ne, which was thought to be closely related to Ne_2^* desorption[9]. In order to confirm the desorption of Ne_2^*, we have measured the spatial distribution of the emitted VUV photons from the desorbed particles initiated by the creation of the surface and bulk excitons.

Experiments have been done at the beam line BL5B in UVSOR. The experimental setup is schematically shown in fig.1, which is similar to the one used in our previous work[3] equipped with a pin hole camera in order to observe the spatial distribution of the emitted light. Briefly, the sample substrate is a Pt(111) attached to the head of a rotatable liquid He cryostat installed in an UHV chamber (base pressure $< 10^{-8}$ Pa). The pin hole camera consists of a MCP with 75mm in diameter, two dimensional position sensitive detector, and a pin hole with 5mm in diameter. The distance between the sample and the pin hole is 90mm and the magnification is unity.

Figure 2 shows a typical image of the spatial distribution of the emitted VUV light from the desorbed excited particles measured at the excitation energy of the 1st order bulk exciton (B1, 70.7nm). Photons emitted from the sample are not detected because of a special geometry of the

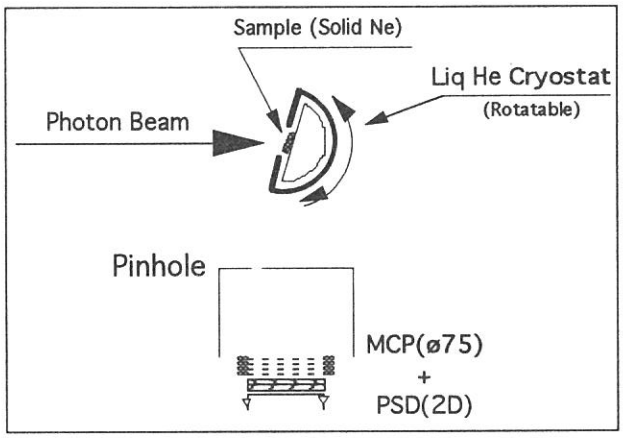

Fig.1. Schematic view of the experimental setup.

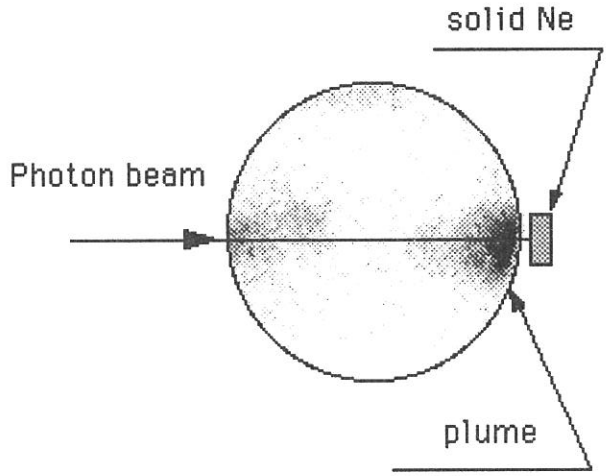

Fig.2. Typical two dimensional image of the spatial distribution of the VUV emission from the desorbed particles from the surface of solid Ne at the excitation of the 1st order bulk exciton (B1, 70.7nm).

* Fax: 03-3987-6732, e-mail: takato.hirayama@gakushuin.ac.jp

experimental setup where the pin hole camera can not directly see the sample surface. The plume, which is observed just in front of the sample surface, is due to the photons emitted from the desorbed particles, and the others are the background signals mainly due to the photons reflected by the chamber wall. From the size of the plume (~15mm) and assuming that the desorbed particle is an excimer with the kinetic energy of 0.23eV which is a calculated result by Chen et al.[5], the radiative lifetime of the desorbed particle is estimated to be about 10μsec. Considering that this value is consistent with the radiative lifetime of the excimer, $Ne_2^*(^3\Sigma_u)$, in the gas phase (11.9μsec)[10], and that the radiative lifetimes of the atomic excited states ($2p^53s$) in the gas phase are in the order of 10^{-9}sec for optically allowed states ($^3P_1$, $^1P_1$), and longer than 10sec for optically forbidden states ($^3P_{0,2}$), we conclude that the plume is due to VUV emissions from the excimer desorbed from the surface of solid Ne. We have done the ESD experiment in Gakushuin University using a similar experimental setup in order to take the decay spectra of the plume intensity, which was not possible in PSD experiment because of very low signal intensity. By using a pulsed electron beam (pulse width ~1μsec, 10kHz repetition) we have obtained time spectra of the plume intensity (not shown). The radiative lifetime measured by the ESD experiment is found to be the same as PSD experiment within an experimental uncertainty.

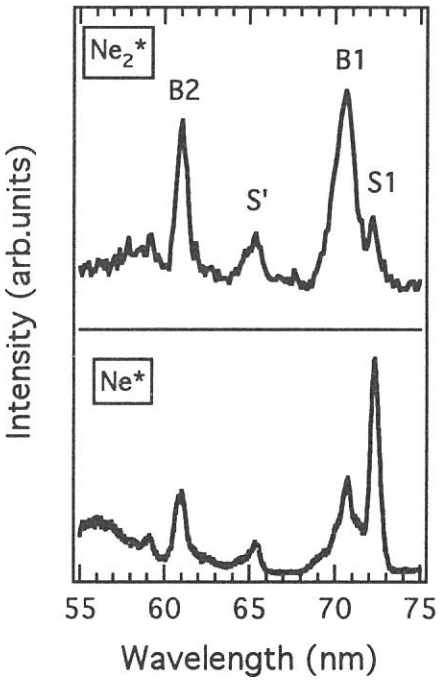

Fig.3. Desorption yield of Ne_2^* and Ne* as a function of wavelength of incident light. Assignments of the surface (S1, S') and bulk (B1, B2) excitons are shown.

Figure 3 shows the plume intensity, i.e., the desorption yield of $Ne_2^*(^3\Sigma_u)$, as a function of wavelength of the incident light together with the result for Ne* desorption[1] from the surface of solid Ne. The spectra show that the excimer desorption is also stimulated by the exciton creation on the surface and in the bulk as in the case of excited atom desorption. The main difference in the excimer desorption compared to the atomic desorption is the decrease of the relative intensity of the 1st order surface exciton (S1, 72.3nm). This can be due to the less number of the nearest neighbor atoms on the surface compared to the bulk, and the efficient desorption of excited atoms on the surface, both of which result in the decrease of the efficiency of the excimer formation on the surface. It is interesting to note that the relative intensity of $2p^53p$-type surface exciton (S', 65.4nm) remains almost constant compared to those of bulk intensities. We do not have a clear explanation for this result at present. Further PSD and ESD experiments are in progress.

References.

[1] T. Hirayama, A. Hayama, T. Koike, T. Kuninobu, I. Arakawa, K. Mitsuke, M. Sakurai and E. V. Savchenko, Surf. Sci. **390**, (1997) 266.
[2] T. Hirayama, T. Nagai, M. Abo, I. Arakawa, K. Mitsuke and M. Sakurai, J. Electr. Spectr. Rel. Phen. **80**, (1996) 101.
[3] I. Arakawa, D. E. Weibel, T. Nagai, M. Abo, T. Hirayama, M. Kanno, K. Mitsuke and M. Sakurai, Nucl. Instrum. Meth. Phys. Res. B**101**, (1995) 195.
[4] T. Kloiber and G. Zimmerer, Radiat. Eff. Def. Solids **109**, (1989) 219.
[5] L. F. Chen, G. Q. Huang and K. S. Song, Nucl. Instrum. Meth. Phys. Res. B **116**, (1996) 61.
[6] S. T. Cui, R. E. Johnson, C. T. Reimann and J. W. Boring, Phys. Rev. B **39**, (1989) 12345.
[7] W. T. Buller and R. E. Johnson, Phys. Rev. B **43** (1991) 6118.
[8] C. T. Reimann, W. L. Brown, D. E. Grosjean and M. J. Nowakowski, Phys. Rev. B **45** (1992) 43.
[9] E. V. Savchenko, T. Hirayama, A. Hayama, T. Koike, T. Kuninobu, I. Arakawa, K. Mitsuke and M. Sakurai, Surf. Sci. **390**, (1997) 261.
[10] B. Schneider and J. H. Cohen, J. Chem. Phys. **61**, (1974) 3240.

(BL6A2) The interaction of Diamond (100) surface with gas particles

N. Takagi, T. Kubo, M. Z. Hossain, S. Hasegawa, T. Aruga and M. Nishijima,

Department of Chemistry, Graduate School of Science, Kyoto University, Kyoto 606

Diamond is promising as an electronic-device material superior to Si or GaAs owing to intrinsic properties such as the large band gap, high saturation carrier velocity and high thermal conductivity. The recent development in the epitaxial growth methods of diamond promotes a number of researches from both fundamental and technological points of view. One of the most important themes is the microscopic understanding of the epitaxial growth mechanism. Although several models are proposed, as far as we know, clear solution for this problem has not been given. It is important to understand the chemical reactivity of the diamond surfaces in order to answer this. From the technological points of view, diamond is a suitable candidate for a negative electron affinity (NEA) device, since its large band gap of $\sim$ 5.5 eV makes the conduction band minimum lie close to the vacuum level. It is well known that the adsorption of alkali metal atoms on solid surfaces induce marked decrease of the work function. In that point of view, the alkali-adsorbed diamond surfaces have a potential to be used as NEA devices.

We have investigated the electronic states of C(100)(2x1)-H and C(100)(2x1), the adsorption of CO on C(100)(2x1) and the adsorption of alkali metals (K and Cs) on C(100)(1x1)+streak. In this report, we present these results.

The B-doped diamond films were grown epitaxially, by using the microwave plasma-assisted chemical vapor deposition (CVD) method, on the (100) surface of synthesized single-crystalline diamond (Ib type). The growth condition is described in ref. [1].The size of the surface was 4x4x0.3mm^3. The CVD-grown diamond surface was H-terminated, and hence the clean surface was obtained by heating the sample up to 1400 K. The clean surface shows the sharp (2x1) low energy electron diffraction (LEED) pattern. The (2x1)-H surface was prepared by exposure of the sample to H atoms produced by a hot W filament ($\sim$1800 K).

The normal emission spectra of the C(100)(2x1)-H surface were measured with the incident photon energy, hv, of 30-70 eV. Peaks at -1.2 and -4.0 eV relative to Fermi level were observed for hv = 40 eV. The peak positions depend on hv reflecting dispersion, and hence these are related to bulk states. After the sample was heated up to 1400 K and H adatoms were fully removed, normal emission spectra of the clean C(100)(2x1) surface were measured (hv = 35-50 eV). For hv = 50eV, a peak related to surface states is observed at -1.8eV. This peak is overlapped with the bulk emission and is not separately observed for hv = 35-40 eV. When the clean surface was exposed to atomic H, the intensity of the peak at -1.8 eV is gradually decreased and finally is disappeared for the (2x1)-H surface. Therefore, this peak is associated with the dangling bond π surface state. The angular resolved spectra of C(100)(2x1) were also measured with hv = 50 eV and the incidence angle of 45 degrees from the surface normal. The dangling bond π surface state shows little dispersion. These results are in good agreement with the results of Graupner et al. [2] for a natural type II-b diamond (100) surface.

When the clean surface was exposed to 1000 L (1L = 1x10^{-6} Torr s) CO at 180 K, normal emission spectra for CO-exposed surface were measured with hv = 35-50 eV. The difference spectra between those for the clean and CO-exposed surfaces were analyzed in detail, but no evidence of CO adsorption on the C(100)(2x1) surface was obtained. The interaction of the other gas molecules (O_2, C_2H_2, N_2O) with C(100)(2x1) has been studied

(experiments were carried out at Kyoto University), but the C(100)(2x1) surface is not reacted with these gas molecules. The chemical reactivity of the C(100)(2x1) surface is very low.

The adsorption of K and Cs on the C(100)(1x1)+streak surface has been studied at room temperature. The work function change ($\Delta\phi$) has been measured by the threshold of the secondary electron as a function of the coverage of alkali atom which is determined by the area intensity of the K 3p and Cs 4d emission. $\Delta\phi$ of -3.0 and -3.3eV are obtained for K and Cs, respectively. The work function change of semiconductor surfaces is generally composed of the adsorbate-induced changes in both band bending and electron affinity. The band bending was not observed for K- and Cs-covered surface and the vacuum level lies close to the conduction minimum for the C(100)(2x1) surface (The electron affinity of the C(100)(2x1) surface is estimated to be 0.8 [3]) , and hence the electron affinity of alkali-covered diamond surfaces is negative.

This work was supported in part by Grants-in-Aid from the Ministry of Education, Science, Sports and Culture, and Sumitomo Electric Industries, Ltd.

Reference

[1] T. Tsuno, T, Imai, Y. Nishibayashi, K. Hamada and N. Fujimori, Jpn. J. Appl. Phys. 30 (1991) 1063.
[2] R. Graupner, M. Hollering, A. Ziegler, J. Ristein, L. Ley and A. Stampfl, Phys. Rev. B55 (1997) 10841.
[3] Z. Chang, M. Wensell and J. Bernholc, Phys, Rev. B51 (1995) 5291.

(BL6A2,BL2B1)

SRPES study on surface core-level shift for GaP(001)-(2×4)

N. Sanada, S. Mochizuki, M. Shimomura, Y. Suzuki, G. Kaneda, T. Takeuchi, N. Utsumi, and Y. Fukuda

Res. Inst. Electronics, Shizuoka University, Hamamatsu 432-8061, Japan.

The surface structure of III-V semiconductors is of interest because it affects the electric properties of III-V semiconductor devices. It is well known that III-group metal-stabilized (001) surfaces of GaAs, InAs, and InSb show a (4×2) or c(8×2) reconstruction with 4× periodicity in the [1$\bar{1}$0] direction[1]. The surface structure has three Ga-(or In-) dimers with a missing dimer in a (4×2) unit cell, obeying electron counting model concept[2]. On the other hand, it is recently suggested by ion scattering measurements that Ar ion bombardment and annealing (IBA) treatments of a GaP (001) surface result in a Ga-stabilized (2×4) reconstruction with 4× periodicity along the [110] direction[3]. The X-ray photoelectron diffraction and STM results also support the above structure[4]. The surface structure of the Ga-stabilized GaP(001)-(2x4) surface is not understood yet in detail. In this study, we present for the first time the surface core-level shift of the Ga 3*d* line for the GaP(001) surface, and discuss the surface structure of GaP(001)-(2×4).

The clean n-GaP(001) surface was obtained by Ar ion bombardment(500V) and annealing at 450°C under 3×10^{-8} Pa. Low energy electron diffraction (LEED) shows (2×4) spots. Photoemission spectra were obtained with a hemispherical energy analyzer. A photon energy of 67 eV was used to enhance the surface sensitivity in the SRPES study.

Figure 1 shows Ga 3*d* SRPES spectra collected from the clean GaP(001)-(2×4) surface at θ=0°, 60°, and 80° along the [110] direction. The spectra can be fitted by three spin-orbit doublet components. The components having a lower binding energy by 0.5 eV and a higher binding energy by 0.4 eV than that of bulk are found. The intensity of the former increases as increases in θ and that of the latter keeps almost constant. On the basis of the energy shift and polar angle dependence of these components, the former peak would originate from topmost surface gallium atoms bonded to other gallium atom. The latter peak is suggested to be due to the gallium atoms with a dangling bond near the surface. The previous model for GaP[2] can not explain both the results of the surface core-level shift and STM observation[4,5]. The new model will be presented on the basis of the result of the surface core-level shift and STM.

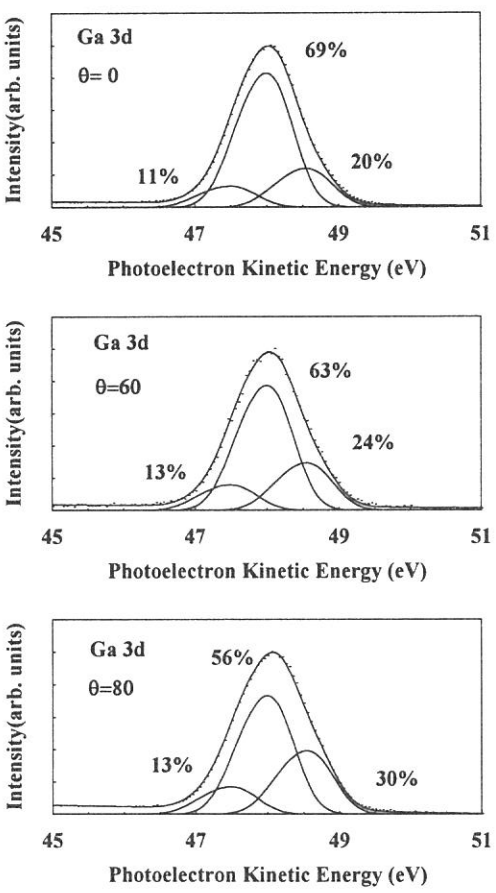

Fig. 1. Ga 3*d* photoemission data acquired at 0°, 60°, and 80°. The three best-fit spin-orbit doublets are shown with solid lines.

References

[1] P.R.Varekamp, et al., Surf. Sci., **350** L221 (1996).
[2] M.D.Pashley, Phys. Rev. B **47**, 10481 (1989).
[3] M.M.Sung and J.W.Ravalais, Surf. Sci., **365**, 136 (1996).
[4] in preparation.
[5] N. Sanada, et al., Appl. Phys. Lett., **67**, 1432 (1995).